Quantification of System Strength from Grid-Forming Resources Using Frequency-Domain Scans

September 2026

AEMO
AUSTRALIAN ENERGY MARKET OPERATOR

We acknowledge the Traditional Custodians of the land, seas and waters across Australia. We honour the wisdom of Aboriginal and Torres Strait Islander Elders past and present and embrace future generations.

We acknowledge that, wherever we work, we do so on Aboriginal and Torres Strait Islander lands. We pay respect to the world's oldest continuing culture and First Nations peoples' deep and continuing connection to Country; and hope that our work can benefit both people and Country.

AEMO is proud to have launched its Innovate Reconciliation Action Plan (RAP) in June 2026. Pictured left and featuring on the cover of the Innovate RAP is Wiradjuri artist Lani Balzan's 'Journey of unity: AEMO's Reconciliation Path', a visual representation of our ongoing journey towards reconciliation – a collaborative endeavour that honours First Nations cultures, fosters mutual understanding, and paves the way for a brighter, more inclusive future.

Important notice

Purpose

Under section 49(1)(e) of the National Electricity Law and Chapter 4 of the National Electricity Rules AEMO is responsible for maintaining and improving power system security. AEMO has prepared this document to provide information about the use of a frequency-domain method for quantifying the system strength support provided by grid-forming inverter-based battery energy storage systems (GFM BESS) and synchronous condensers (SynCon). This work forms part of a broader suite of initiatives aimed at developing the evidence base to improve AEMO's technical understanding of the services and capabilities needed to maintain power system security as the NEM transitions to a low or zero emissions power system, and supports one of AEMO's Engineering Roadmap FY2026 Priority Actions (Quantifying System Strength Support from Grid-Forming Technologies (ID FY26_24)). This document is based on information available to AEMO as at 1 July 2025, unless otherwise stated.

AEMO is currently engaging with proponents, TNSPs and other stakeholders through relevant industry forums to support trials of the method, seek additional feedback and undertake further testing across a broader range technologies, network conditions, operating points and system strength issues to confirm its broader applicability. Future progress will be communicated through AEMO's Engineering Roadmap publications and relevant stakeholder forums.

Disclaimer

This document and the information in it:

- is provided for information only;
- does not constitute legal, business, engineering or other technical advice;
- may be subsequently updated or amended;
- is not intended to, and does not, affect, alter or limit AEMO's, TNSP's or any participant's obligations under the National Electricity Law or National Electricity Rules, or any other applicable laws, procedures or policies; and
- should not be relied on as a substitute for obtaining detailed advice about the National Electricity Law, the National Electricity Rules (NER), or any other applicable laws, procedures or policies or the capability or performance of relevant equipment.

AEMO has made reasonable efforts to ensure the quality of the information in this document but cannot guarantee its accuracy or completeness. Accordingly, to the maximum extent permitted by law, AEMO and its officers, employees and consultants involved in the preparation of this document:

- make no representation or warranty, express or implied, as to the currency, accuracy, reliability or completeness of the information in this document; and
- are not liable (whether by reason of negligence or otherwise) for any statements or representations in this document, or any omissions from it, or for any use or reliance on the information in it.

Copyright

Executive summary

Frequency-domain analysis can quantify the system strength support provided by a specific grid-forming (GFM) plant or synchronous condenser (syncon) and estimate the capacity required to remediate an identified system strength issue. This could improve early-stage option assessment and reduce the number of iterative electromagnetic transient (EMT) simulations required, potentially saving time and cost for proponents, network service providers (NSPs) and AEMO.

The approach could provide valuable information for project developers to undertake an early assessment of likely remediation options and costs, allowing them to make an informed decision on the most appropriate connection pathway.

Project-specific EMT validation remains necessary, and AEMO will continue testing the method across a broader range of devices and system conditions while seeking stakeholder feedback on its benefits.

This report proposes and tests a frequency-domain method for quantifying the system strength support provided by GFM battery energy storage systems (BESS) and syncons.

This work forms part of AEMO's Engineering Roadmap program to build the evidence base for earlier, more efficient and transparent assessment of emerging system strength solutions, with potential benefit for proponents, NSPs and AEMO, as the power system transitions to higher levels of inverter-based resources (IBRs).

The method uses the frequency-domain characteristics of each device to assesses how closely the device behaves like an ideal voltage source. Based on this assessment, AEMO derived a numerical indicator of dynamic system strength support for the studied devices. This method complements EMT time-domain studies, by establishing a robust baseline for targeted analyses, and offers an efficient, unified framework for quantifying system strength in IBR-dominated power systems.

System strength is the measure of power system's ability to maintain and control the voltage waveform (stable magnitude and phase angle) at any node in the network, both during steady state operation and following a disturbance[1]. It is critical to enable stable operation of IBRs, particularly grid-following (GFL) IBRs, which rely on the presence of a strong grid. Rotating machines, such as coal-fired synchronous generators, have been the main system strength providers in the power system to date. As the ageing coal-fired synchronous generation fleet gradually retires, and the energy transition progresses with more IBRs coming onto the grid, the need for other devices capable of providing system strength services has been growing.

One proven technology for replacing synchronous generators in the provision of system strength services is the syncon. GFM BESS have recently emerged as a viable alternative provider of stability-related system strength solutions, and have demonstrated capabilities in maintaining a stable voltage waveform.

[1] 2025 *Transition Plan for System Security*, https://www.aemo.com.au/-/media/files/major-publications/tpss/2025-transition-plan-for-system-security.pdf.

AEMO and transmission network service providers (TNSPs) are further exploring opportunities to leverage grid-forming capabilities to meet the growing system strength requirements for stable voltage waveforms[2,3,4,5].

There is an increasing need to identify, quantify and compare alternative sources of system strength support. Existing EMT-based approaches typically start from an identified system strength issue, such as unstable inverter response or unacceptable voltage waveform behaviour under defined operating conditions. They then test different remediation options through repeated time-domain simulations until a suitable solution is found. This process typically requires validated EMT models, controller settings, network assumptions and plant design information that may not be available during early assessment. When multiple technology options, locations, ratings and tuning assumptions must be compared, the assessment effort can grow significantly.

Through the Engineering Roadmap[6], AEMO is proactively seeking new and efficient ways to quantify critical system support services provided by GFM plants, including synthetic inertia[7] and system strength services, to pave the way for a wider adoption of this critical piece of technology into Australia's future power systems. In AEMO's *Voluntary Specification for Grid-Forming Inverters*[8], GFM plants' voltage source behaviour is a core capability required from all GFMs, which enables their ability to provide system strength. In AEMO's recent analysis of an IBR-driven sub-synchronous oscillation[9], the analysis adopted a frequency-domain analysis to identify the source of the oscillation during a weak-grid operation condition, without the use of extensive time-domain EMT analysis.

Leveraging on this existing work, this report presents a different, and potentially more efficient and transparent, approach to compare system strength support options. Through this new approach, the system strength contribution of different devices may be quantified using numerical values known as dynamic short-circuit ratio (dSCR) values which are derived based on the frequency-domain transfer functions of the devices. These dSCR values are directly proportional to the system strength support capability of these devices.

For the purposes of this report, the term dSCR provides a dynamic representation of stable voltage waveform characteristics, and can still work with the conventional short circuit ratio (SCR) terms, when addressing a specific system strength problem, such as identifying the sizing requirement for a GFM device or syncon to remediate the identified system strength problem. Throughout this report, the term "dSCR" is used as an analytical metric; it is not defined in the National Electricity Rules (NER) and does not affect or alter AEMO's, NSPs' or participants' obligations under the National Electricity Law or NER.

The analysis using the proposed quantification method shows that system strength support from GFM BESS can vary materially between designs and tuning settings. It also indicates that a single device may provide different levels of support

[2] Victorian System Strength Requirement regulatory investment test for transmission (RIT-T) Project Assessment Conclusions Report (PACR), https://www.vicgrid.com.au/__data/assets/pdf_file/0033/772377/victorian-system-strength-requirement-rit-t-pacr.pdf.

[3] Meeting system strength requirements in New South Wales RIT-T PACR, https://www.transgrid.com.au/media/kfhd21bq/250812-transgrid-system-strength-pacr.pdf.

[4] Addressing System Strength Requirements in Queensland from December 2025 PACR, https://www.powerlink.com.au/sites/default/files/2025-07/Addressing%20System%20Strength%20Requirements%20from%20Dec%202025%20-%20PACR%20-%20June%202025.pdf.

[5] System Strength Requirements in South Australia RIT-T Project Specification Consultation Report (PSCR), https://electranet.com.au/wp-content/uploads/2024/11/ElectraNet-System-Strength-RIT-T-PSCR-FINAL.pdf.

[6] See https://www.aemo.com.au/initiatives/major-programs/engineering-roadmap.

[7] Quantifying Synthetic Inertia of a Grid-forming Battery Energy Storage System – Technical Note, https://www.aemo.com.au/-/media/files/initiatives/engineering-framework/2024/quantifying-synthetic-inertia-from-gfm-bess.pdf.

[8] Voluntary Specification for Grid-forming Inverters, aemo.com.au/-/media/files/initiatives/primary-frequency-response/2023/gfm-voluntary-spec.pdf.

[9] See https://www.aemo.com.au/-/media/files/initiatives/engineering-framework/2025/analysis-of-sub-synchronous-oscillation-in-west-murray-zone-power-system-in-australia---external.pdf.

for the active- and reactive-power dynamics. The resulting dSCR values are therefore specific to the device design, control settings, operating conditions and network context.

For the specific configurations assessed in this report, the syncon produced higher dSCR values than the two GFM BESS projects considered. The dSCR values presented in this report are specific to the models, configurations and tuning assessed and should not be generalised as representative values for a technology type. The proposed method provides a pathway for a case-by-case assessment of different device capabilities using transparent assumptions and appropriate validation.

The work undertaken supports the use of the method described in this report as an early-stage screening and indicative sizing tool, subject to undertaking project-specific EMT studies for final validation. The approach accurately estimated the minimum required grid SCR to stabilise wind farm for each assessed system strength device, including two GFM BESS and one syncon, to within 5% of corresponding values derived from the time-domain EMT simulations.

The analysis provides confidence that the system strength support from different devices can be quantified using a unified method, with numerical indicators that can compare the system strength capabilities using arithmetic calculation. The application of this method may provide valuable insights for project developers through the provision of consistent numerical indicators for technology comparison, preliminary remediation sizing, and cost assessment. This can support more informed decision-making regarding the most appropriate connection pathway and the scope of targeted EMT studies.

AEMO is now engaging with proponents, TNSPs and other stakeholders through relevant industry forums to support trials of the method and seek additional feedback. Further testing across a broader range of GFM designs, syncon configurations, network conditions, operating points and system strength issues will confirm its broader applicability. Future progress will be communicated through AEMO's Engineering Roadmap – which going forward will be incorporated in AEMO's *Transition Plan for System Security* annual publication – and relevant stakeholder forums.

Contents

Tables

Figures

1 Introduction

The objective of this work is to develop and demonstrate a frequency-domain approach for quantifying system strength support from a system strength device (SSD). In this report, SSDs refer to GFM BESS and syncons. According to AEMO's *Voluntary Specification for Grid-forming Inverters*[10], GFM inverters are expected to "stably operate in remote and weak parts of the grid, without support from nearby synchronous machines, noting that all limits should be respected. The stiff voltage reference of a GFM inverter during power system disturbances should also improve the stability of nearby GFL inverters". This requirement is also applicable to a syncon.

This work is motivated by the increasing need to assess system strength support options efficiently and consistently as the power system transitions toward higher levels of IBRs. The system strength support provision from SSDs has been proven by many existing analyses[11]. However, most existing approaches used EMT time-domain simulation. These studies are essential for detailed assessment and validation, but they can be simulation-intensive when used to compare multiple device types, ratings, tuning assumptions and operating conditions. While such studies reveal the positive correlation between the size of a SSD device and the amount of system strength support provided by this device, they fail to quantitatively evaluate the amount of system strength provision by different SSD technologies.

In addition, when using EMT time-domain simulation, the size of SSD required to resolve an existing system strength deficit can only be determined iteratively through a trial-and-error approach via a series of repeated simulations with different SSD sizes. This adds on to the already very extensive simulation time described above for assessing the effectiveness of the SSD. This approach also depends on an existing system strength deficit already being identified in the time-domain simulation which would only happen after detailed analysis. This process is necessary for detailed validation, but it can be time-consuming and may require detailed models, controller settings and network assumptions that are not available during early connection or remediation assessment.

Traditional SCR, based on fault-level calculations, can provide an early indication of system strength conditions. However, conventional SCR does not directly quantify the dynamic voltage-source behaviour of SSDs, nor does it directly indicate how much dynamic support a specific GFM BESS or syncon may provide under a given operating condition. A complementary metric is therefore needed to estimate SSD support requirements, compare technology options and serve as a screening tool to guide targeted EMT validation studies.

This report proposes a frequency-domain, quantitative approach to estimate the required size of SSDs to provide system strength support, intended to support earlier and more transparent comparison of SSD capability, while recognising that detailed EMT studies remain necessary for final validation of specific remediation options.

This work aims to:

- develop a frequency-domain approach to quantify system strength support from SSDs using EMT models,
- define and demonstrate numerical metrics for comparing the dynamic system strength support provided by GFM BESS and syncons under the studied assumptions,

[10] At https://aemo.com.au/-/media/files/initiatives/primary-frequency-response/2023/gfm-voluntary-spec.pdf.

[11] For example, Powerlink published study reports on this topic, at https://arena.gov.au/knowledge-bank/pscad-assessment-of-the-effectiveness-of-grid-forming-batteries/.

- apply the proposed metrics for quantifying system strength improvement delivered by SSDs, or to determine the SSD capacity required to enhance the resilience of GFL resources against small-signal instabilities, such as sub-synchronous oscillations, and
- use the quantified support requirements to guide targeted follow-on EMT studies to validate the adequacy of the mitigation measure in addressing both small-and large-signal instabilities.

The work documented in this report falls under the Priority Action "Quantifying system strength support from grid-forming inverters" (ID FY26_24) outlined in the Engineering Roadmap FY2026 Priority Actions report[12]. It is therefore part of a broader suite of initiatives aimed at developing the evidence base to improve AEMO's technical understanding of the services and capabilities needed to maintain power system security as the NEM transitions to a low or zero emissions power system.

1.1 Relationship to system strength framework in the NEM

The *National Electricity Amendment (Efficient management of system strength on the power system) Rule 2021 no. 11* amended the NER's system strength framework to establish a system strength standard under NER S5.1a.9[13], comprising a minimum three-phase fault level, and a separate requirement for stable voltage waveforms at connection points, also known as the efficient level of system strength. These requirements provide the formal framework for identifying and planning system strength needs in the power system. This report focuses on efficient level of system strength component.

The method proposed in this report is not intended to replace the existing system strength framework or the detailed studies required for compliance and connection assessment. Instead, it is intended to provide a complementary analytical approach for comparing the dynamic system strength support capability of different SSDs. In particular, the frequency-domain method may support earlier comparison of remediation options, estimate indicative SSD sizing requirements, and focus subsequent EMT studies on a smaller set of credible solutions. This would reduce the number of iterative EMT simulations required and improve assessment efficiency for stakeholders.

By providing a numerical indicator of dynamic support capability, the method would help bridge the gap between early-stage fault-level-based screening and detailed EMT validation. This would support more efficient assessment of system strength remediation options, while maintaining the need for detailed case-specific validation using appropriate network models, plant models and agreed study assumptions.

1.2 Report structure

This report consists of three major sections:

- Section 2 describes the theoretical basis of the frequency-domain approach used to quantify system strength support from GFM BESS and syncons. It explains how targeted EMT simulations are used to derive device response characteristics and how these characteristics are translated into numerical indicators of dynamic system strength support.

[12] At https://www.aemo.com.au/-/media/files/initiatives/engineering-framework/2025/engineering-roadmap-fy2026-priority-actions-report.pdf?rev=e99db0d3c01543d584e25df0df6936ad&sc_lang=en&hash=3A887388D4A850FC99A59B9A0D9D227E.

[13] At https://energy-rules.aemc.gov.au/ner/803/873790#S5.1a.9.

- Section 3 applies the proposed method to quantify the system strength support provided by two GFM BESS projects and one syncon installed in the National Electric Market (NEM) under the studied assumptions. The section compares the assessed devices using the proposed metrics and discusses how device design, tuning and dynamic response characteristics affect the quantified support capability.
- Section 4 applies the quantified SSD support metrics to two case studies involving system strength-related instability mechanisms. The case studies examine how the proposed approach can inform initial remediation sizing and reduce reliance on repeated trial-and-error EMT simulations during early assessment, while retaining targeted EMT studies for validation of the final mitigation performance.
- Section 5 presents conclusions, and Appendix A1 provides the derivation and additional analysis of the frequency-domain system strength quantification method.

2 Methodology

This section describes the frequency-domain methodology used in this report to quantify dynamic system strength support from SSDs. The methodology is based on comparing the frequency-domain response of each SSD with the response of an ideal voltage source behind an impedance, using a common technical basis called system strength Jacobian. The system strength Jacobian captures the relationship between changes in voltage magnitude and angle, and the corresponding active power and reactive power response of the SSD. Appendix A1 presents the derivation of the system strength Jacobian.

2.1 A new metric for system strength: dynamic short-circuit ratio (dSCR)

The frequency-domain response of system strength Jacobian provides a benchmark for interpreting how closely the SSD behaves like a voltage source over the relevant frequency range. The frequency-domain response of the system strength Jacobian is also used to derive the dSCR, which is used in this report as an indicator of the SSD's dynamic system strength capability.

In this way, the system strength Jacobian provides a common reference for assessing the voltage-source-like behaviour of SSDs, while the dSCR translates that behaviour into a practical metric for comparing the level of dynamic system strength support provided by different devices.

In summary, the method comprises three steps:

- derive the system strength Jacobian of an SSD from frequency-domain scans,
- obtain the dSCR values from selected transfer functions in the frequency-domain magnitude response of the system strength Jacobian, and
- use the dSCR values to compare the SSD's system strength capability and support the assessment of selected instability mitigation cases.

As an example, **Figure 1** shows the frequency-domain magnitude response of the system strength Jacobian for an ideal voltage source behind an impedance. The impedance is considered to have a resistance R = 0.075 ohm (Ω), and an inductance L = 0.72 millihenry (mH), while the peak phase voltage of the voltage source is V_1 = 0.56 kilovolts (kV). This voltage source behind an impedance configuration represents an SCR of 2 condition, based on 1 MVA and 0.69 kV[14] system bases.

[14] Root Mean Square (RMS) voltage = $0.56 \times \sqrt{3/2} = 0.69\ kV$

Figure 1 **Frequency-domain magnitude response of the system strength Jacobian for an ideal voltage source behind reactance – Figures 1(b) and 1(d) show the gain and phase of reactive power response to voltage magnitude perturbations ($Q/V_m(s)$), Figures 1(a) and 1(c) show the gain and phase of active power response to voltage angle expressed on the voltage-equivalent basis as ($P/(V_1 \cdot \theta(s))$)**

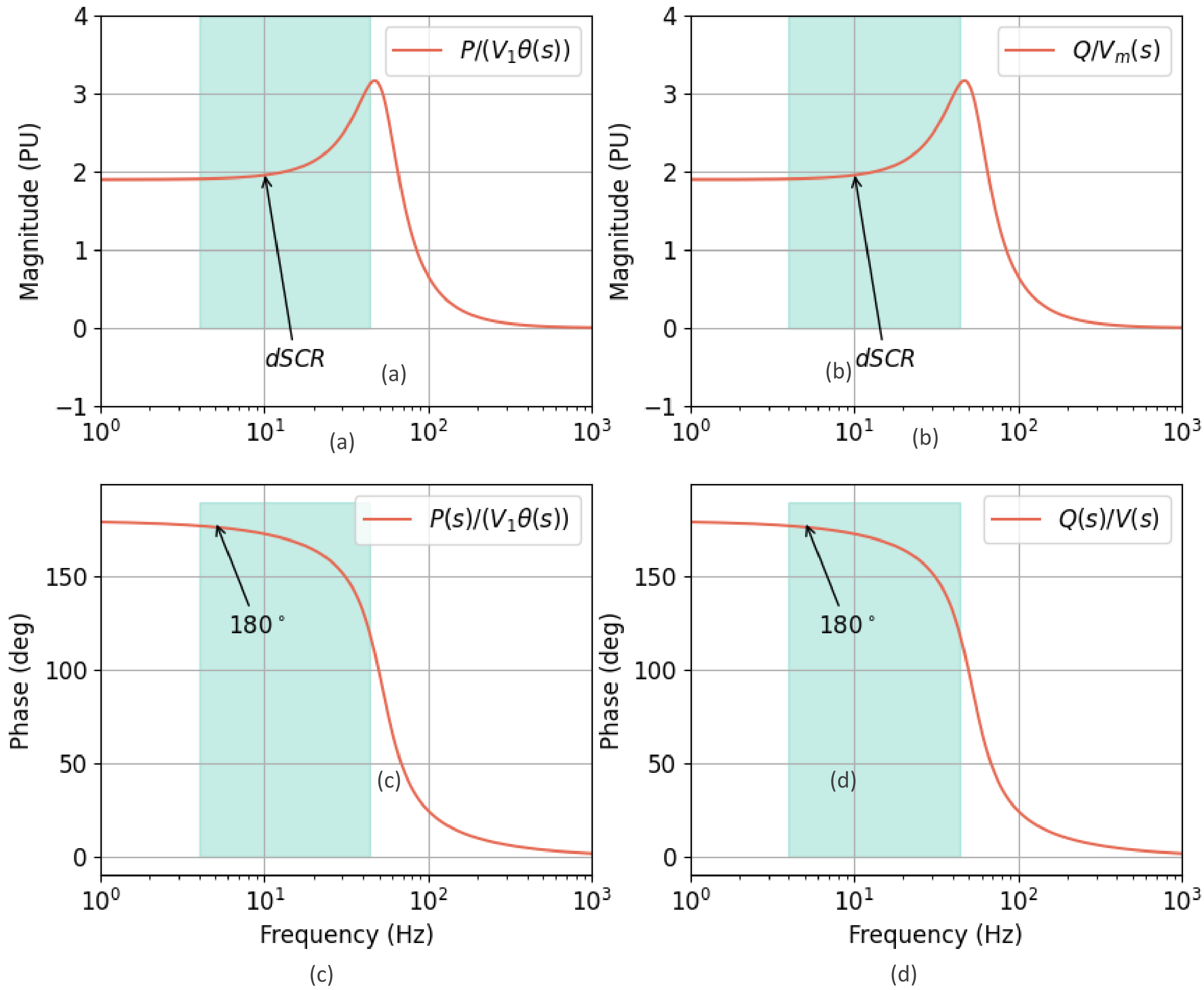

For the ideal voltage source benchmark, the per-unit magnitude of the relevant transfer functions in the system strength Jacobian in the sub-synchronous frequency range is comparable to the SCR value used to define the voltage source impedance. As shown in **Figure 1(b)**, the gain of reactive power response to voltage magnitude perturbations ($Q/V_m(s)$) in the sub-synchronous frequency range (plotted in per unit terms using the system base values mentioned before) is around 2, which is the same as the SCR value of 2 of the ideal voltage source used in the benchmark analysis. Further, as shown in **Figure 1(a)**, the gain of active power response to voltage angle expressed on the voltage-equivalent basis as ($P/(V_1 \cdot \theta(s))$) in the sub-synchronous frequency range (plotted in per unit terms using the system base values mentioned before) is around 2, which is again the same as the SCR value of 2 of the ideal voltage source used in the benchmark analysis. Further, as shown in **Figure 1(c)** and **Figure 1(d)**, the phase is approximately 180 over this frequency range, indicating that the voltage source opposes changes in voltage magnitude and phase, thereby contributing to system strength.

The $Q/V_m(s)$ and $P/(V1 \cdot \theta(s))$ transfer functions are used because they represent the main direct relationships between voltage perturbations and power response in the system strength Jacobian. They therefore provide a basis for comparing the dynamic system strength support capability of different SSDs. Appendix A1 has further analysis of the frequency-domain response of the system strength Jacobian.

2.2 Case study procedure

This report documents a few case studies to demonstrate the application of the proposed system strength quantification method. The study procedure undertaken in this work included two parts, described as follows:

- Part 1 (see Section 3) quantified the system strength support provided by each assessed SSD. For each device, the relevant frequency-domain responses were derived and the dSCR values obtained. This provides a common benchmark for comparing the system strength support capability of different SSDs. Section 3 presents the application of this quantification method to three SSDs: two GFM BESS projects and one syncon. The results are used to compare their dynamic system strength support capability under the studied assumptions.
- Part 2 (see Section 4) applied the dSCR-based quantification method to selected weak-grid instability cases involving an IBR. The dSCR values were used to estimate the level of system strength support required from the SSD to improve stability for the studied cases. This application is intended to reduce reliance on repeated trial-and-error EMT simulations for initial sizing. However, the method does not remove the need for targeted EMT validation where required. Section 4 demonstrates two examples where different system strength-related instability mechanisms are assessed and mitigated, using the SSD quantification method described earlier.

3 Part 1: Quantification of system strength provision

This section applies the frequency-domain quantification method described in Section 2 to obtain dSCR values of the assessed SSDs. The devices were selected because project-specific EMT models were available for the analysis, allowing the proposed method to be demonstrated using models representative of actual projects. The assessed devices differ in original equipment manufacturer (OEM) technology, rating, connection voltage and project-specific design, control and tuning characteristics. The assessed devices are:

- a 150 megavolt amperes (MVA) GFM BESS connected at 66 kV, referred to as GFM BESS Project 1,
- a 30 MVA GFM BESS connected at 132 kV, referred to as GFM BESS Project 2, and
- a 25 MVA synchronous condenser connected at 66 kV, referred to as syncon.

For each SSD, the relevant frequency-domain responses are derived from the impedance scan results at the Point of Connection (PoC). These responses are converted into the two dSCR values defined in Section 2:

- $dSCR_{QV}$ based on the magnitude of the Q/Vm(s) transfer function, and
- $dSCR_{P\theta}$ based on the magnitude of the P/θ(s) transfer function

These values provide a common basis for comparing the dynamic system strength support capability of the assessed SSDs under the study assumptions. The dSCR values are normalised on each SSD's own MVA rating, and they should be interpreted as indicators of support capability per unit of device rating. The absolute physical support provided at the PoC also depends on the size of the device and the connection voltage. This key difference will be further explained in Section 4, where the effectiveness of these SSD to mitigate a specific system strength risk is discussed.

Throughout this report, "dSCR" and "dSCR values" are used for analytical purposes; these terms are not defined or used in the NER and nothing in this report is intended to affect, alter or limit AEMO's, NSPs' or any participant's obligations under the National Electricity Law or NER.

3.1 System strength quantification for GFM BESS Project 1 and Project 2

Project 1

The Bode plot of the $Q/V_m(s)$ transfer function of Project 1 is shown in **Figure 2**, which is derived from impedance scan results obtained at the PoC of the GFM BESS following the methodology described in Section 2. For illustration purposes, both **Figure 2(a)** and **Figure 2(b)** show the frequency-domain characteristics of the $Q/V_m(s)$ transfer function of Project 1, with **Figure 2(a)** showing the transfer function magnitude in real Var/Volt terms, while **Figure 2(b)** shows the per unit terms. The same notation is used for all subsequent plots in this section.

For an SSD with voltage-source-like behaviour, the magnitude plot of the $Q/V_m(s)$ bode plot remains relatively constant/flat within the frequency range of interest, and the phase is closer to 180 degrees. As shown in **Figure 2(a)**, a frequency point (@4.8 hertz [Hz]) gives the amount of Var/Volt provided by Project 1 at its connection point, within the 4-40 Hz frequency range, where the Q/V_m(s) bode plot magnitude response remains relatively flat. As Project 1 is connected to a 66 kV bus, it provides 7065 Var/Volt at the 66 kV connection point. The bottom plot of Figure 2(a) shows the phase of the Q/V_m(s). The phase remains relatively flat within -120 to -180 degrees range. The phase jump to 180 degrees, seen around 10 Hz in the bottom plot of **Figure 2(a)**, is due to phase wrapping applied during plotting.

As shown in **Figure 2(b)**, 7065 Var/Volt at the 66 kV connection point can be represented as 2.53 per unit (pu)/pu[15] when converted based on Project 1 rating of 150 MVA and the peak value of the phase voltage at the connection point voltage[16]. The per-unit Q/V_m ratio of 2.53 pu/pu is therefore defined as the dSCR of the Q/V_m transfer function on its own rating ($dSCR_{QV}$)[17] which can be used as one metric to quantify the grid strength contribution from Project 1 at its PoC (66 kV).

Figure 2 The frequency-domain model of Q/V of a GFM BESS from Project 1

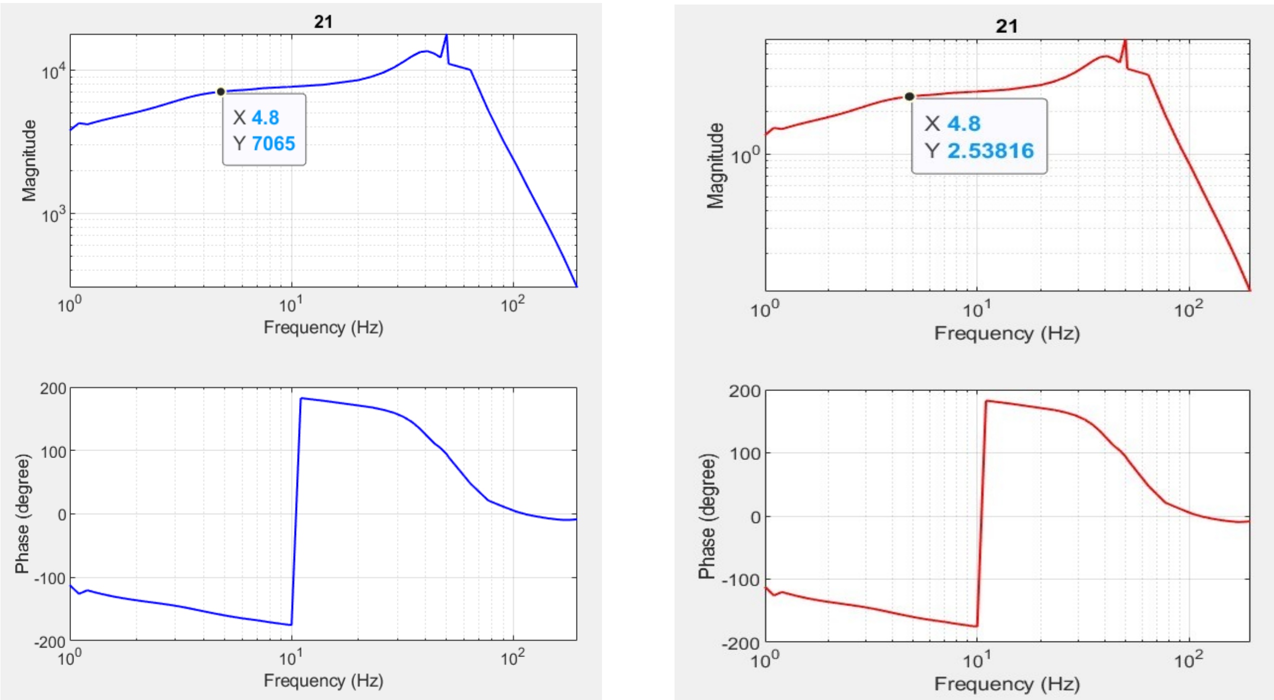

(a) (b)

Similarly, **0** shows the P/θ(s) transfer function of the same Project 1 derived using the same methodology. **0(a)** shows the magnitude (upper plot) and the phase angle (lower plot) of the P/θ(s) transfer function, with the magnitude ratio expressed in Watts/radian. From the magnitude plot in **0(a)**, it can be seen the P/θ(s) transfer function of Project 1 also exhibits a constant/flat magnitude profile, within the frequency range of 2-40 Hz, indicating the voltage source behaviour of the Project 1 within this frequency range. As defined previously, the dSCR of P/θ ($dSCR_{Pθ}$) is expressed in a per unit ratio, based on Project 1 MVA rating, which is calculated to be 2.91 pu/pu[18], as shown in **0(b)**.

[15] Per-unitised Var/Volt amount = $7065 \times (53900/150000000) = 2.53\ pu/pu$

[16] Per-phase peak value of 66 kV connection point = $66 \times \sqrt{2/3}\ kV = 53.9\ kV$

[17] ESIG Webinar, "Nilesh Modi and Shahil Shah, 2025, *Analysis of IBR-driven Oscillations in the Australian Grid*", at https://www.esig.energy/event/webinar-analysis-of-ibr-driven-oscillations-in-the-australian-grid/.

[18] Per-unitised Watt/Radian amount = $436962000 \times (1/150000000) = 2.91\ pu/pu$

When assessing the system strength contribution of Project 1, the lower value between $dSCR_{QV}$ and $dSCR_{P\theta}$ should be used. However, a specific value, either $dSCR_{QV}$ or $dSCR_{P\theta}$, may be used when assessing the effectiveness of Project 1 when providing system strength support to remediate a specific oscillation mechanism manifested in either reactive or active power dynamics of a GFL IBR, respectively. This is further discussed in Section 4.

Figure 3 The frequency-domain model of P/ θ of a GFM BESS from Project 1

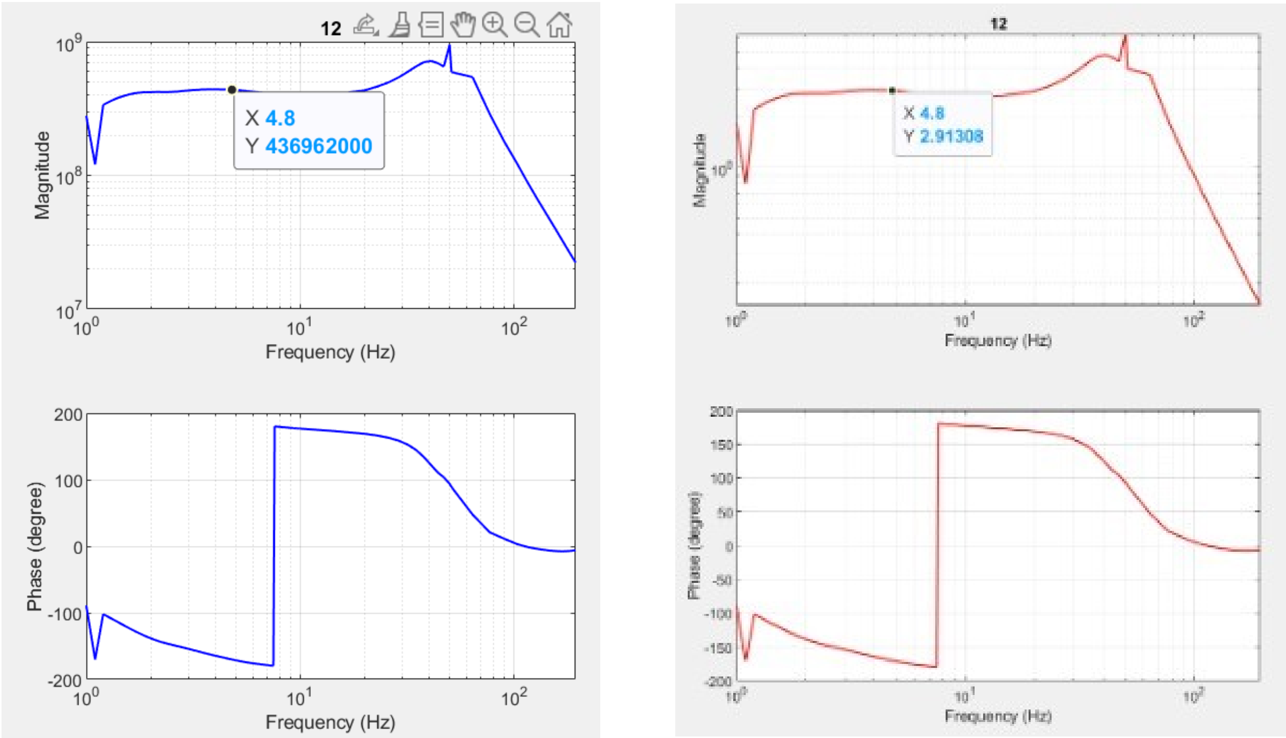

(a) (b)

Project 2

Figure 4 shows the Bode plot of the $Q/V_m(s)$ transfer function of a Project 2. Similar to Project 1, a frequency point (@10 Hz) in the magnitude plot of the $Q/V_m(s)$ within the 4-20 Hz frequency range is considered, as shown in **Figure 4(a)**. This data point suggests Project 2 provides an equivalent voltage source behaviour of 1 kilovolt amperes reactive (kVar)/Volt at the 132 kV connection point, within the frequency range of 4-20 Hz. As shown in **Figure 4(b)**, 1 kVar/Volt at the 132 kV connection point is equal to 3.71 pu/pu[19] when converted to per unit based on its own rating of 30 MVA and the peak value of the phase voltage of the connection point voltage: 108 kV[20]. Therefore, the $dSCR_{QV}$ for Project 2 is 3.71 pu/pu.

[19] Per-unitised Var/Volt amount = $1040.57 \times (108000/30000000) \cong 3.71\ pu/pu$

[20] Per-phase peak value of 66 kV connection point = $132 \times \sqrt{2/3}\ kV = 108\ kV$

Figure 4 The frequency-domain model of Q/V of a GFM BESS from Project 2

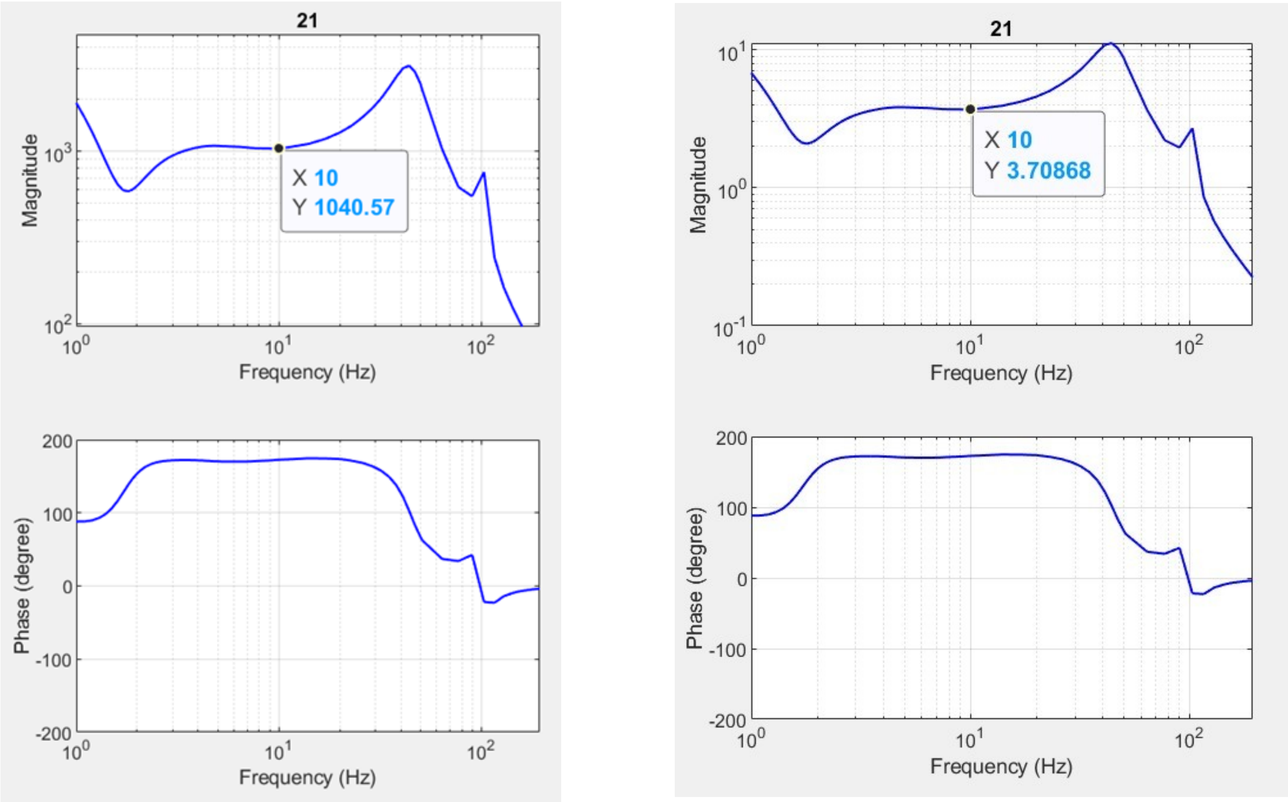

(a) (b)

Figure 5 shows the Bode plot of the P/θ(s) transfer function of Project 2. Compared with the magnitude plot of the $Q/V_m(s)$ bode plot shown in **Figure 5(a)**, **Figure 5(a)** shows a narrower frequency range where Project 2 demonstrates a constant/flat magnitude profile in the P/θ(s) bode plot, that is, approximately 10-20 Hz compared with 4-20 Hz shown in the $Q/V_m(s)$ bode plot. This suggests Project 2 can provide equivalent voltage source behaviour in a smaller frequency range for active power dynamics, compared with reactive power dynamics. The $dSCR_{P\theta}$ for Project 2 is calculated to be 5.99[21], as shown in **Figure 5(b)**.

[21] Per-unitised W/Radian amount = $179927000 \times (1/30000000) = 5.99\ pu/pu$

Figure 5 The frequency-domain model of P/ θ of a GFM BESS from Project 2

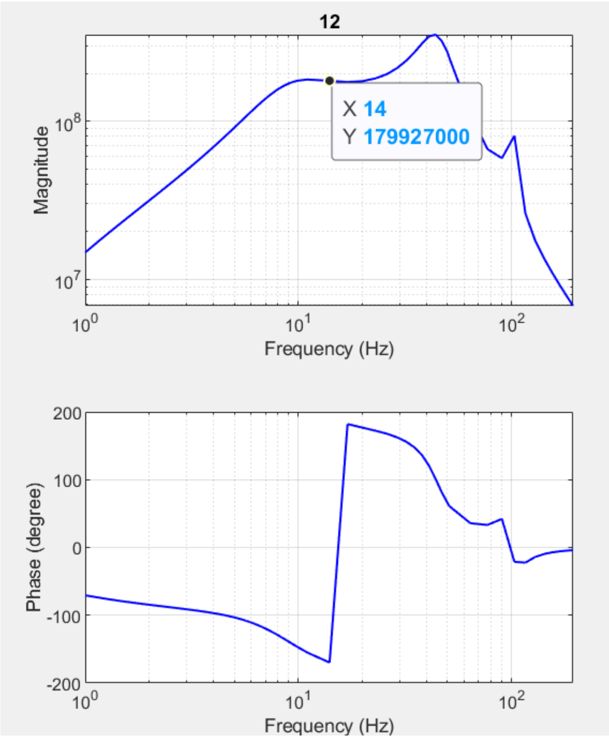

(a)

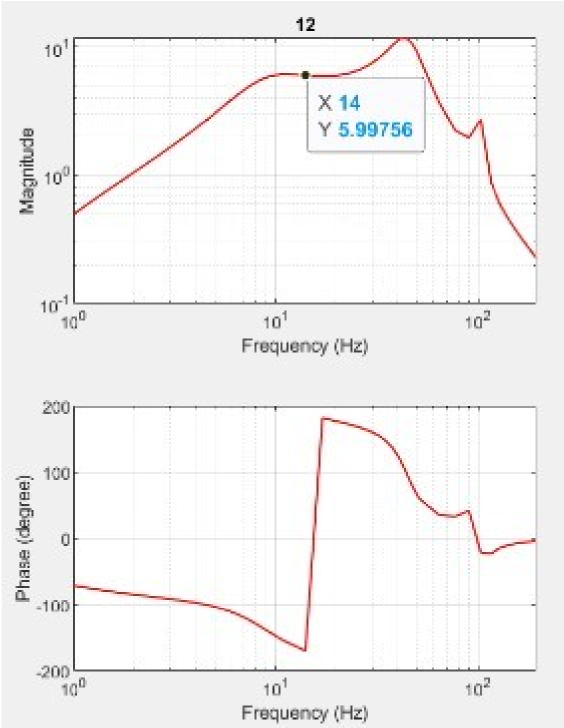

(b)

3.2 System strength quantification for a syncon

Figure 6 shows the Bode plot of the $Q/V_m(s)$ transfer function of a 25 MVA syncon. As shown in **Figure 6(a)**, the syncon provides 2.4 kVar/Volt at the 66 kV connection point. As shown in **Figure 6(b)**, 2.4 kVar/Volt at the 66 kV connection point is equal to 5.3 pu/pu[22] when converted to per unit based on its own rating of 25 MVA and the peak value of the phase voltage at the connection point: 53.9 kV[23]. Therefore, the $dSCR_{QV}$ for the synchronous condenser is 5.3 pu/pu, currently calculated at a frequency point of 4.2 Hz.

Figure 7 shows the Bode plot $P/\theta(s)$ transfer function of the SynCon, with the $dSCR_{P\theta}$ value calculated as 7.28[24] as shown in **Figure 7(b)**, calculated at a frequency point of 10 Hz.

[22] Per-unitised Var/Volt amount = $2400 \times (53900/25000000) = 5.2\ pu/pu$

[23] Per-phase peak value of 66 kV connection point = $66 \times \sqrt{2/3}\ kV = 53.9\ kV$

[24] Per-unitised W/Radian amount = $182140000 \times (1/25000000) = 7.28\ pu/pu$

Figure 6 The frequency-domain model of Q/V of a synchronous condenser

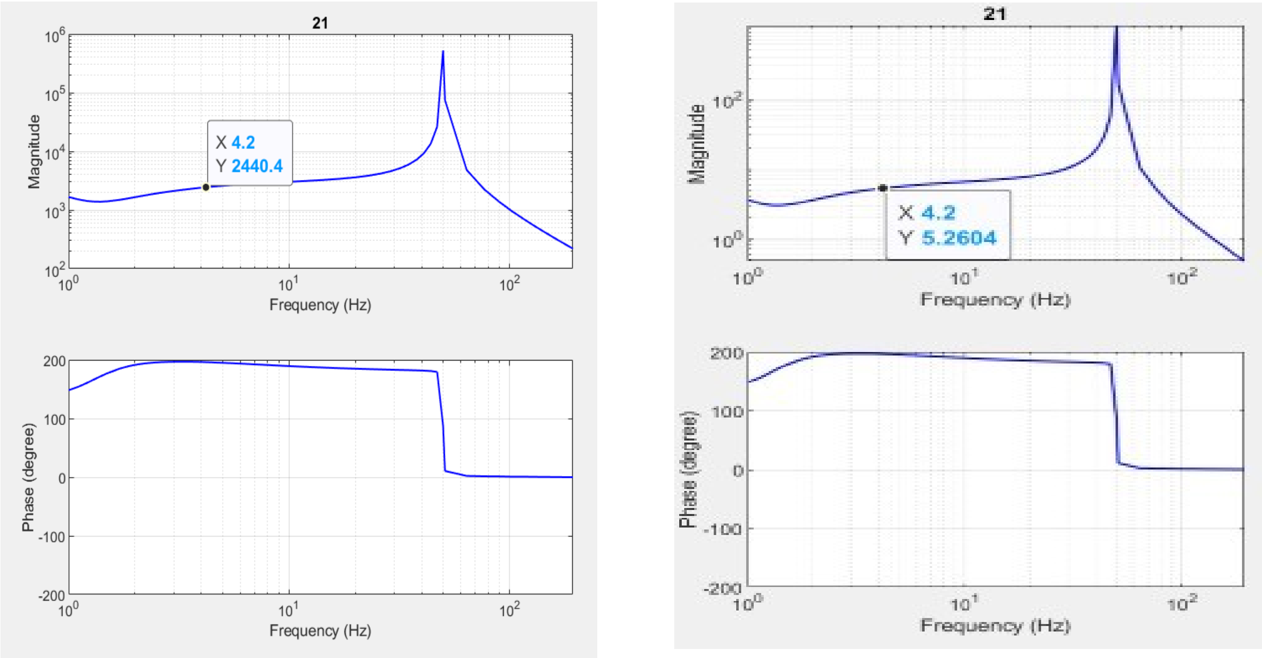

(a) (b)

Figure 7 The frequency-domain model of P/ θ of a synchronous condenser

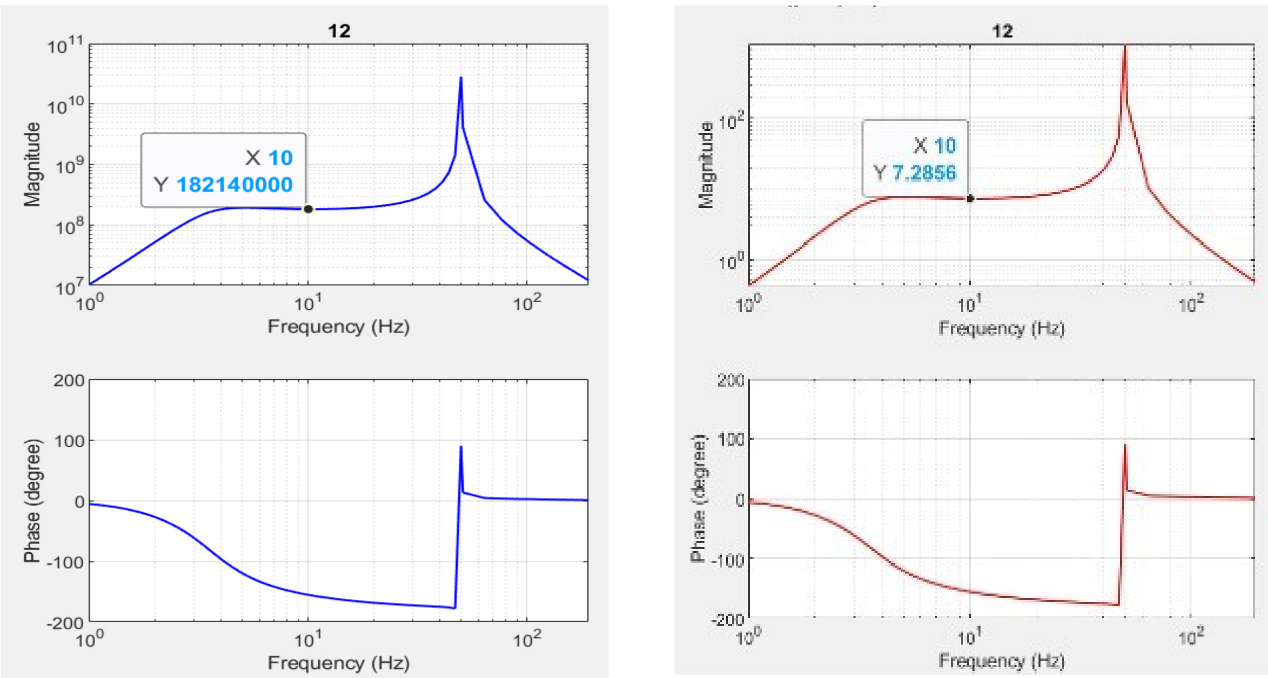

(a) (b)

3.3 Summary of the Q/V(s) and P/θ(s) support provided by each SSD

Table 1 summarises the system strength support provided by each SSD at their corresponding connection point based on their own rating. As described in Section 2, for each SSD two dSCR values are derived based on different transfer functions, representing different system strength support capability of the same SSD, to support active (with $dSCR_{P\theta}$) and reactive power (with $dSCR_{QV}$) dynamics.

The frequency points where the dSCR values are measured are also presented in **Table 1**. For each SSD and transfer function, the reported dSCR is the lowest gain within the frequency range where each SSD's voltage source behaviour can be realized. Both dSCR values and the frequency range where SSD's voltage source behaviour is realized are important. This provides a consistent basis for comparing the system strength support provided by the assessed SSDs across that frequency range, and should not be interpreted as a comparison of device response at a single common frequency or at every frequency within the band.

Table 1 Summary of system strength provided by each SSD under studied assumptions

SSD	Size of the SSD	$dSCR_{QV}$ (pu/pu)	$dSCR_{P\theta}$ (pu/pu)
GFM BESS Project 1	150 MVA	2.53 @ 4.8 Hz	2.91 @ 4.8 Hz
GFM BESS Project 2	30 MVA	3.71 @ 10.0 Hz	5.99 @ 14.0 Hz
Synchronous condenser	25 MVA	5.30 @ 4.2 Hz	7.28 @ 10.0 Hz

As shown in **Table 1**, under the studied configurations and selected evaluation frequencies, the syncon had higher dSCRs for both active and reactive power dynamic support than both GFM BESS projects. GFM BESS Project 2 had higher dSCRs than GFM BESS Project 1, however it should be noted that the additional benefits can only be realised in a smaller frequency range, particularly when it comes to active power dynamic support.

It should be noted that the results presented in **Table 1** are based on specific GFM BESS and syncon configurations and tuning considered in this report. The results do not demonstrate that one technology type provides superior system strength support to another. Such capabilities must be assessed on a case-by-case basis, using the relevant device model, tuning, operating conditions, connection point and frequency range of interest.

3.4 System strength capability of SSDs for different operating points

The influence of active power operating point variations on the dSCR has been assessed, noting that SSDs may operate at different outputs when they are connected to the grid.

This sensitivity considered two active-power operating points for the GFM BESS projects:

- 1 pu active-power injection, and
- 0 pu active-power injection.

For each active power injection operating point, the system strength Jacobian was calculated, and the corresponding frequency-domain models of the P/θ(s) and Q/V(s) transfer functions derived. The resulting transfer-function frequency responses for GFM BESS Project 1, GFM BESS Project 2, and the synchronous condenser are presented in **Figure 8**. Note that the syncon has only been considered at 0 pu given the lack of a prime mover.

Figure 8 The frequency-domain models of (a) P/θ(s) and (b) Q/V(s) of each SSD for different operating points

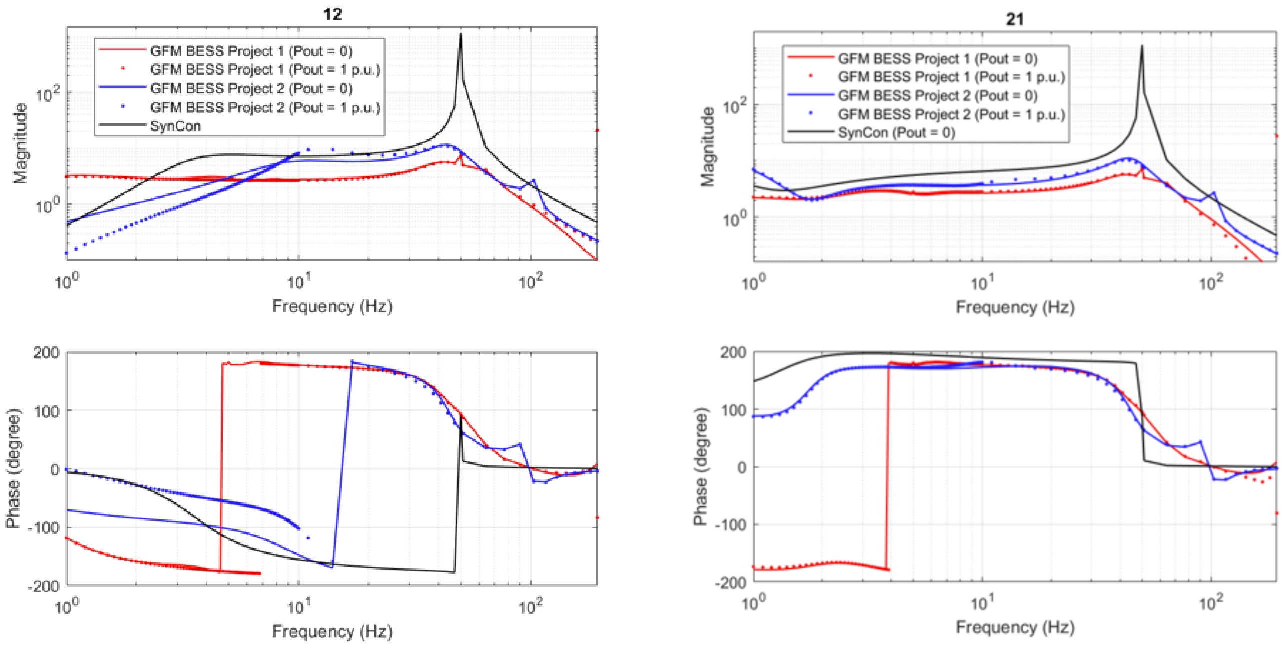

(a) (b)

As shown in **Figure 8**, variations in the active power operating points do not significantly affect the P/θ(s) and Q/V(s) models of SSDs. The responses obtained when the SSD operates at 1 pu active-power injection closely match those obtained when no active power is injected. Multiple active-power operating points were not examined for the synchronous condenser, as it typically does not supply active power to the grid. Consequently, the dSCR contribution from each SSD remains essentially unchanged across the considered operating points.

As described in Section A1.3, dSCR values should be determined for relevant operating points within the SSD's operating envelope, including reactive power output, voltage set points, and potential alternative control modes. Where variation exists, the minimum dSCR contribution over the operating range is used as a conservative estimate.

4 Part 2: Application of stability improvement with SSDs

This section applies the dSCR-based quantification method to two weak-grid instability case studies with GFL IBRs. The first case considered a 200 megawatts (MW) wind farm (WF) connected to a 500 kV transmission network, where the identified instability is primarily associated with reactive-power dynamics. The second case considered a 100 MW solar farm (solar farm) connected to a 66 kV network, where the identified instability is primarily associated with active-power dynamics.

The purpose of these case studies is to demonstrate how the dSCR values obtained in Section 3 can be used to estimate the level of system strength support required to improve stability for the studied cases. The frequency-domain method was used for initial estimation and sizing. Targeted EMT time-domain simulations were then used to validate the predicted stability boundary for the cases assessed.

The analysis followed the following steps:

- Step 1 – identify the minimum stable SCR without SSD support. The minimum stable SCR is the lowest grid SCR at the GFL IBR connection point, for which the IBR remains stable under the studied operating condition. In this section, impedance-based stability analysis was used to identify the minimum stable SCR, and EMT time-domain simulations in PSCAD™ were used for targeted validation.
- Step 2 – identify the dominant instability mechanism and select the corresponding dSCR support. Reduced-order frequency domain analysis was used to identify whether the instability is primarily associated with active or reactive power dynamics. This allows the selection of the corresponding dSCR values from SSD ($dSCR_{P\theta}$ or $dSCR_{QV}$) for each instability mechanism.
- Step 3 – scale the SSC dSCR to IBR plant rating. The dSCR value derived for each SSD in Section 3 was normalised on the SSD's own rating. For the case study, the dSCR values from Section 3 were scaled to match the rating of the GFL IBR generation plant under study ($dSCR_{IBR}$). This conversion quantifies the "effective SCR" contributed by the SSD at the PoC, supplementing any shortfall in the grid's inherent SCR.
- Step 4 – estimate the residual grid SCR requirement. The residual grid SCR required for stability with SSD support is the difference between the minimum stable SCR without SSD determined in Step 1, and the "effective SCR" ($dSCR_{IBR}$) contributed from SSD determined in Step 3.
- Step 5 – sizing the SSD requirement. If the residual grid SCR requirement is calculated to be negative, it is interpreted that SSD contribution exceeds the minimum system strength support requirement for the GFL IBR plant. Otherwise, the required size of an SSD will be determined to ensure the residual grid SCR requirement is no more than the actual grid SCR condition at the targeted connection point of the GFL IBR.

The following sections first discuss the stabilisation of the wind farm followed by the stabilisation of solar farm using the three SSD plants discussed in Section 3.

4.1 Stabilisation of wind farm with reactive power instability

The wind farm considered in this work has a registered capacity of 200 MW at the PoC and is connected to the 500 kV transmission network, as shown in **Figure 9**.

Figure 9 Single-line diagram of wind farm's connection to the grid

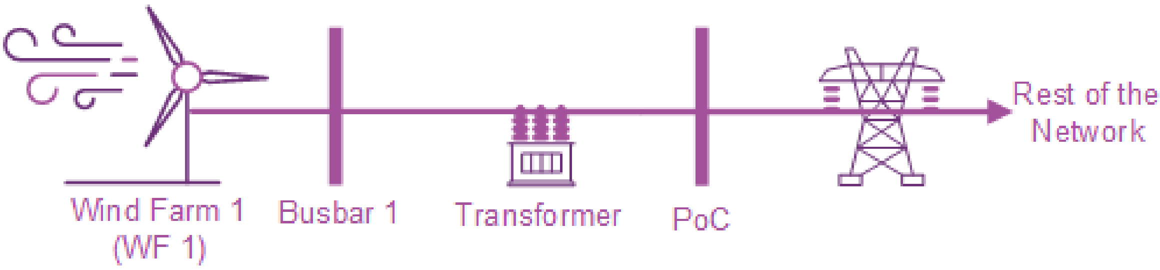

4.1.1 Analysis and identification of the wind farm instability for low SCR conditions

Figure 10 shows the results of the impedance-based stability analysis for the wind farm for an operating point of P_0 = 200 MW and Q_0 = 23 MVar under the grid conditions of SCR = 3 and X/R = 10. The impedance-based stability analysis of the wind farm reveals an instability mode around 5 Hz for a grid SCR below 3. When the grid SCR = 3, the frequency response of $Z_m(s)$ shown in **Figure 10(a)** contains an underdamped resonance mode around 5 Hz when the wind farm is connected to the grid. **Figure 10(b)** shows that the multivariable Nyquist plot is very close to encircling the critical point of (-1,0) around 5 Hz, indicating potential instability.

Figure 10 Stability analysis of wind farm for a grid strength condition of SCR = 3 and X/R = 10

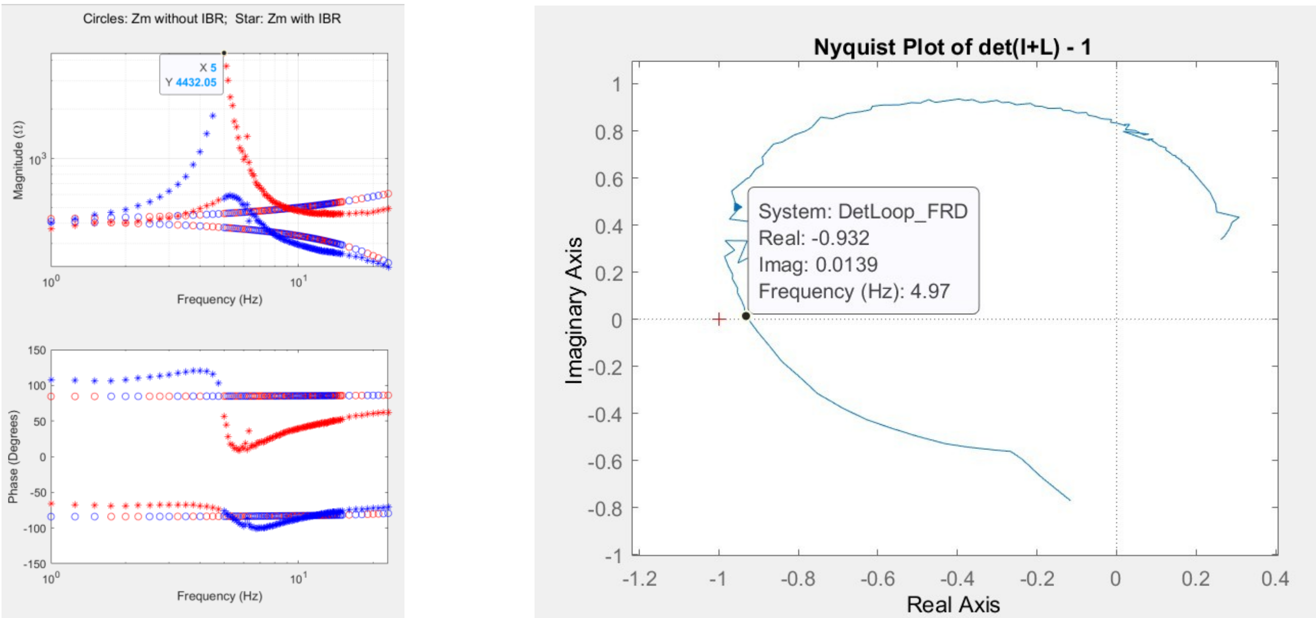

(a) (b)

To further understand the instability observed, reduced-order analysis for active and reactive power dynamics was conducted in DQ domain. In this analysis, the products of the DQ components of the grid impedance ($Znet_{dq}$ and $Znet_{qd}$) and the DQ components of the IBR plant admittance ($Yplant_{dq}$ and $Yplant_{qd}$) are individually considered to identify whether the active or reactive power dynamics dominate the observed mode.

Figure 11(a) shows the Nyquist plot of $Znet_{qd} \cdot Yplant_{dq}$[25], which relates to the active power dynamics and **Figure 11(b)** shows the Nyquist plot of $Znet_{qd} \cdot Yplant_{qd}$[26], which relates to the reactive power dynamics. As shown in **Figure 11(b)**, the very close proximity of the Nyquist plot to the critical point, which is (-1,0), signifies small stability margins around 5 Hz indicating potential instability originating in the reactive power control loop.

Figure 11 Nyquist plot of (a) $Znet_{qd}$*$Yplant_{dq}$ and (b) $Znet_{qd}$*$Yplant_{qd}$

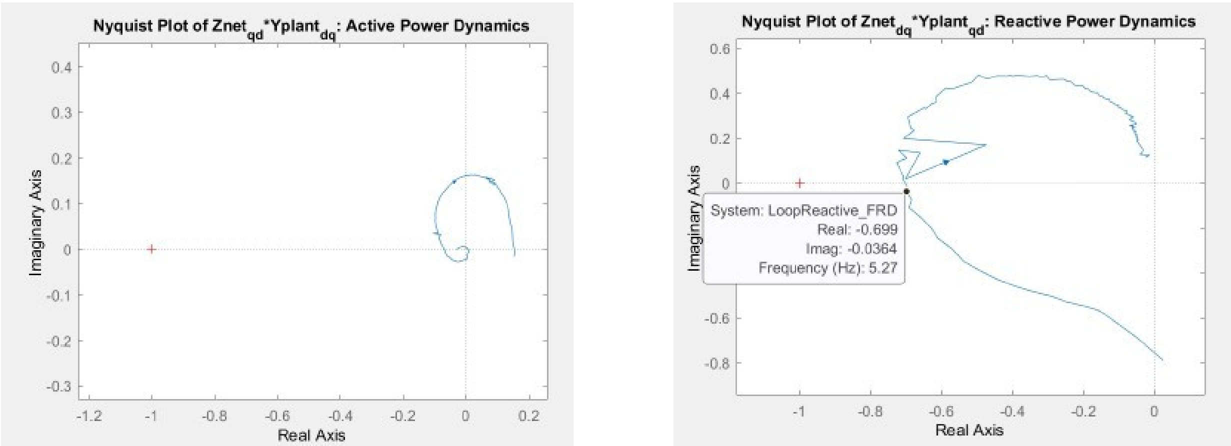

(a) (b)

The findings from the reduced-order analysis are further confirmed by the reduced stability margin, particularly the gain margin (gain difference between grid and wind farm characteristics as phase difference approaches 180 degrees), observed in the admittance response of $Ynet_{qd}$[27] of grid and plant around 5 Hz as shown in **Figure 12**. Therefore, reduced-order analysis shows that the unstable mode at 5 Hz manifests in the reactive power control loop of the wind farm.

[25] "·" refers to scalar multiplication.

[26] "·" refers to scalar multiplication.

[27] Ynetqd = Iq/Vd

Figure 12 The admittance response of Ynetqd = Iq/Vd of grid in black and plant in red

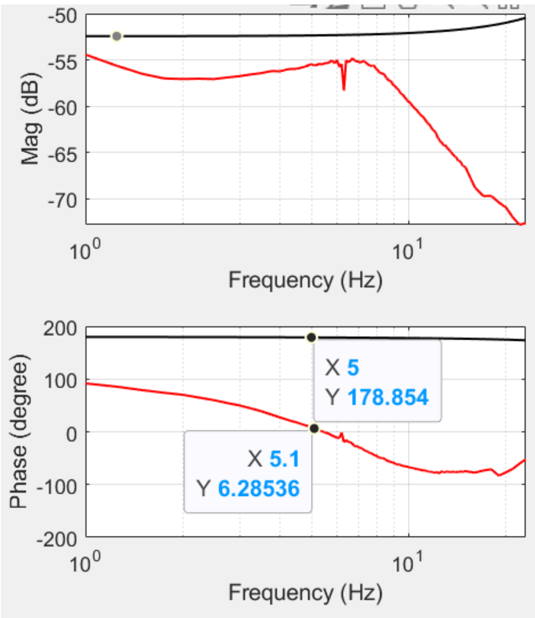

4.1.2 Validation of the identified instability mode in time-domain

The instability mode identified using impedance-based stability analysis is verified using time-domain EMT studies done in PSCAD utilising a single machine infinite bus (SMIB) setup. **Figure 13** shows the results of the time-domain results of the wind farm when the SCR is reduced from 3 to 2.5 at t = 15 seconds (s) in the simulation.

Figure 13 PSCAD™ time-domain simulation results of wind farm when the SCR is reduced to 2.5 from 3

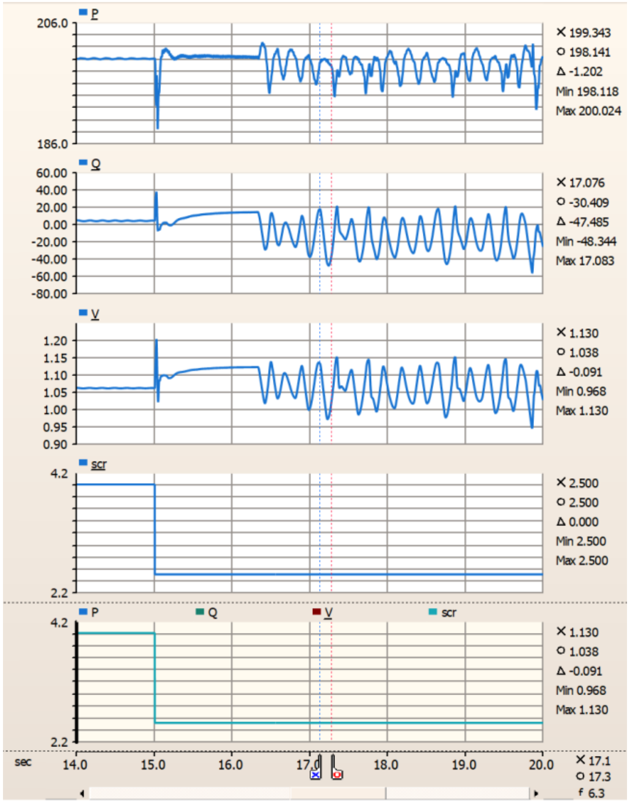

The results suggest that soon following the SCR reduction, the oscillations are seen in wind farm active power, reactive power and voltage from t = 16.5 s. These time-domain results are consistent with the impedance-based analysis, which identified a low-frequency instability mechanism at grid SCR less than 3.

4.1.3 Quantification of system strength improvement by SSD for wind farm

This section applied the two GFM BESS and one syncon discussed in Section 3 to improve the wind farm stability. The minimum SCR level that the wind farm can operate stably was then compared, with different SSD connected in parallel to the wind farm connection point. The single-line diagram of the SSD's connection parallel to wind farm's PoC is shown in **Figure 14**.

Figure 14 Single-line diagram of the SSD's connection in parallel to the wind farm

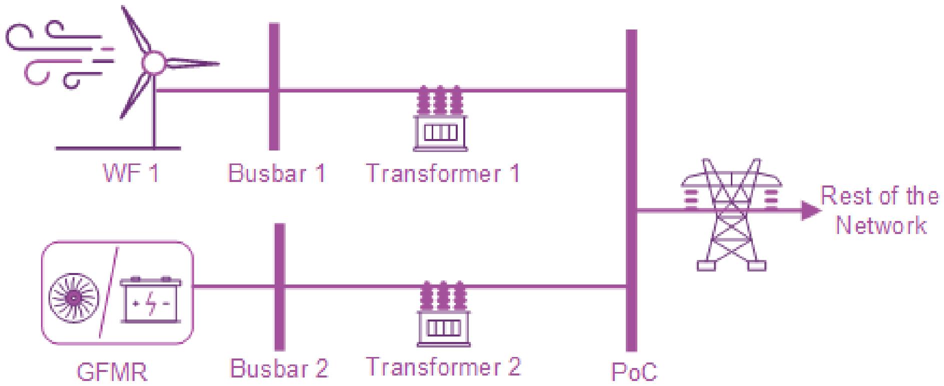

Figure 15 shows the impedance response of $Q/V_m(s)$ of the grid in black and the wind farm in red at the PoC for two different grid SCR levels of 3 and 1.5, respectively. The $Q/V_m(s)$ response is used, instead of $P/\theta(s)$, because the instability mechanism of the wind farm is mainly associated with its reactive power dynamics as identified in Section 4.1.1.

As shown in **Figure 15(a)**, the grid, represented by an ideal voltage source behind an impedance, with an SCR level of 3, would provide 1,470 Var/Volt at the PoC of wind farm which enables the stable operation of the wind farm. However, when the grid SCR is reduced to 1.5, the grid would only provide 736 Var/Volt, as shown in **Figure 15(b)**. For the wind farm to operate stably at such a grid condition, the SSD must supply additional Var/Volt to compensate for the diminished Var/Volt contribution from the grid. In doing so, the SSD increases the effective system strength at the PoC of the wind farm, despite the actual grid SCR being lower.

The SSD contribution should be interpreted as an equivalent dynamic support contribution at the wind farm PoC. It does not change the physical grid SCR, but reduces the residual grid SCR required from the network to ensure wind farm stable operation under the study assumptions.

Figure 15 Q/V for two different levels of grid SCR at the 500 kV PoC of wind farm

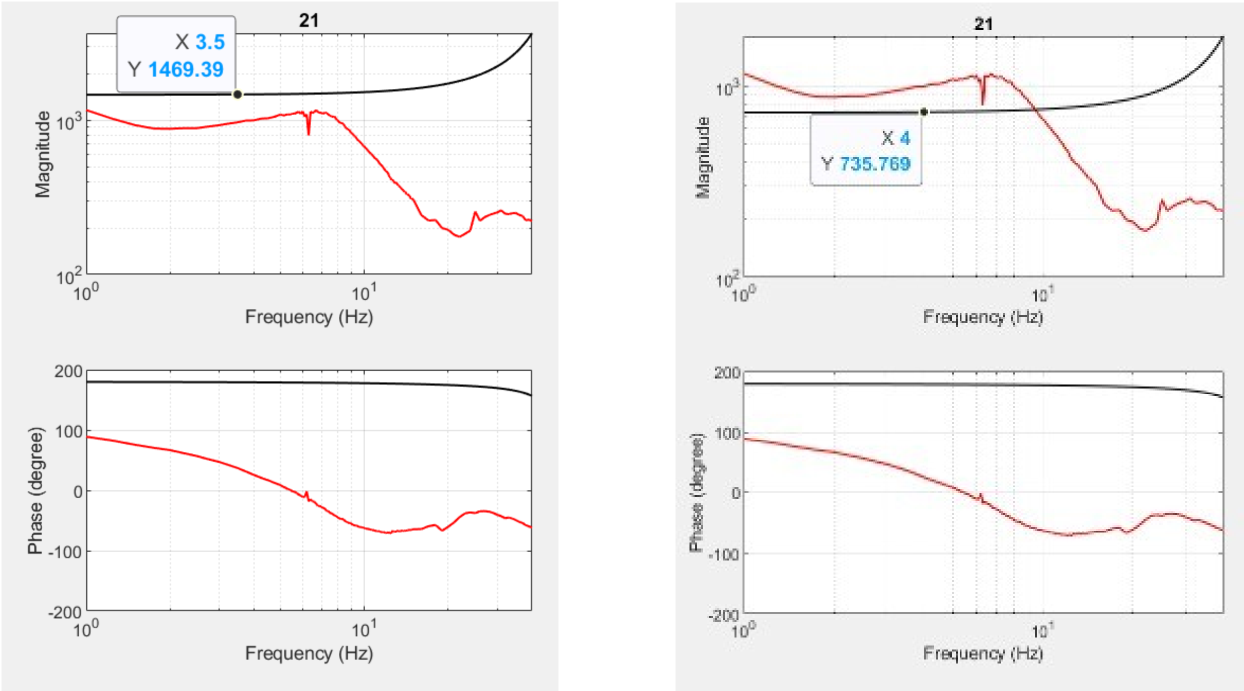

(a) SCR = 3 (b) SCR = 1.5

System strength provided by GFM BESS from Project 1

As shown earlier in **Figure 2**, a 150 MVA GFM BESS from Project 1 provides 7 kVar/Volt at its 66 kV connection point, which is equivalent to 924 Var/Volt at the 500 kV PoC of the wind farm. If a 150 MVA GFM BESS from Project 1 is connected to stabilise the wind farm (which requires a total of 1,470 Var/Volt for stable operation as per **Figure 15**), only 546 Var/Volt[28] needs to come from the grid, which is equivalent to a residual grid SCR of 1.1[29]. Hence, with a 150 MVA GFM BESS from Project 1, the wind farm can operate stably for grids with a SCR level above 1.1, as the GFM BESS from Project 1 is providing a $dSCR_{WF}$[30] of 1.9 based on the rating of the wind farm (this is calculated by simply subtracting 1.1 from the minimum stable SCR for the wind farm, which is 3) at the 500 kV PoC.

Alternatively, $dSCR_{WF}$ can be directly calculated by scaling dSCR, which is 2.53 for GFM BESS from Project 1 on its own rating, to match the capacity of the wind farm rating (200 MW). The relationship between $dSCR_{WF}$ and dSCR is given by:

$$\mathrm{dSCR}_{\mathrm{WF}} = \frac{\textit{Size of the SSD}}{\textit{Capacity of the IBR plant}} \times \mathrm{dSCR}. \tag{4.1}$$

[28] This value is determined by simple arithmetic calculation, by subtracting grid strength provision from GFM BESS of 924 Var/Volt, from the total required grid strength of 1,470 Var/Volt (equivalent to SCR of 3 at wind farm PoC).

[29] The Var/Volt provision from a grid, represented by an ideal source behind an inductance, has a linear relationship with the equivalent SCR. For example, a grid with a provision of 1470 Var/Volt is equivalent to a SCR of 3, therefore a grid condition with 546 Var/Volt is proportionally equivalent to a SCR of 1.1.

[30] System strength provided by the SSD calculated based on wind farm’s rating

In summary, the connection of GFM BESS Project 1 next to the wind farm not only allows the wind farm to operate stably at a grid SCR of 3, where the wind farm would be prone to instability without the GFM BESS, it also allows wind farm stable operation for any grid SCR conditions higher than the residual grid SCR requirement of 1.1.

To validate this sizing practice, **Figure 16(a)** shows the Nyquist plot of the loop gain when the wind farm is connected to a grid SCR of 1.1 alone. Without the GFM BESS, the Nyquist plot indicates instability under the study assumptions, with the plot encircling the -1 point counterclockwise. With the GFM BESS connected, **Figure 16(b)** shows the Nyquist plot no longer encircles the critical point, indicating improved stability margin for this case.

Figure 16 Nyquist plot of the loop gain at SCR 1.1 (a) without a GFM BESS (b) with a GFM BESS from Project 1

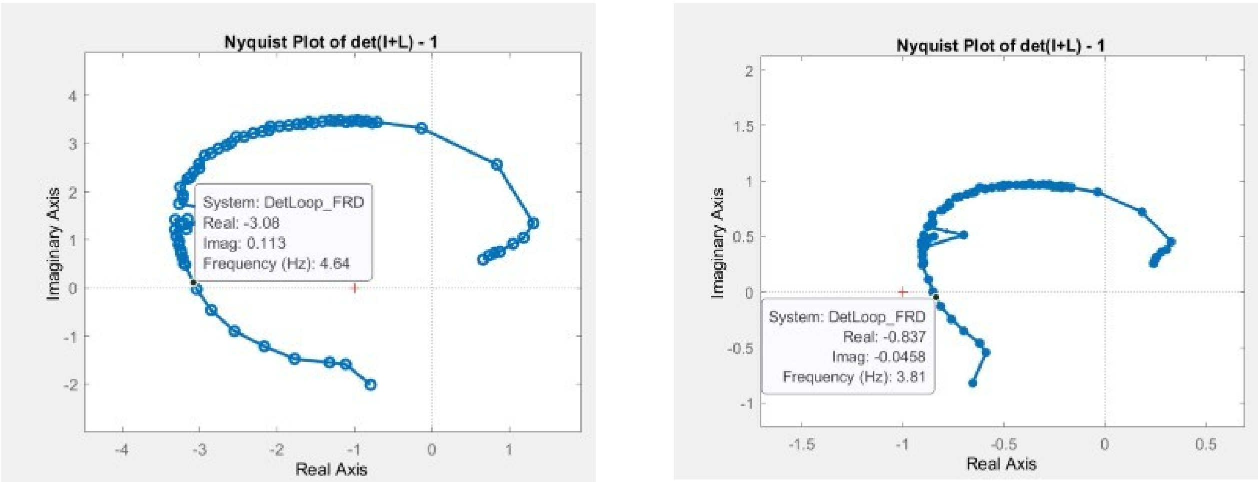

(a) (b)

System strength provided by GFM BESS from Project 2

As shown earlier in **Figure 4**, a 30 MVA GFM BESS from Project 2 provides 1,000 Var/Volt at its 132 kV connection point, which is equivalent to 264 Var/Volt at the 500 kV PoC of the wind farm. Similar to the analysis done for GFM BESS from Project 1, if a 30 MVA GFM BESS from Project 2 is connected to stabilise the wind farm (which requires a total of 1,470 Var/Volt for stable operation), 1206 Var/Volt needs to come from the grid, which is equivalent to a grid SCR of 2.45. Hence, when a 30 MVA GFM BESS from Project 2 is connected in parallel to stabilise the wind farm, stable operation is expected for grid SCR levels above 2.45, as the GFM BESS from Project 2 is providing a $dSCR_{WF}$ of 0.55 at the 500 kV PoC, scaled from a $dSCR_{QV}$ value of 3.71 based on 30 MVA, as listed earlier in **Table 1**.

System strength provided by a synchronous condenser

As shown earlier in **Figure 6**, a 25 MVA syncon provides 2,400 Var/Volt at its 66 kV connection point, which is equivalent to 317 Var/Volt at the 500 kV PoC of the wind farm. If the 25 MVA syncon is connected in parallel to stabilise the wind farm (which requires a total of 1,470 Var/Volt for stable operation), only 1,153 Var/Volt needs to come from the grid, which is equivalent to a grid SCR of 2.35. Hence, with the 25 MVA syncon connected in parallel to the wind farm, stable operation of the wind farm can occur for a grid SCR level above 2.35, as the syncon provides a $dSCR_{WF}$ of 0.65 at the 500 kV PoC.

Table 2 provides a summary of the dSCR and $dSCR_{WF}$ provided by each SSD and the minimum grid SCR level that the wind farm can stably operate at with each SSD connected.

Table 2 Summary of the dSCR provided by each SSD to stabilise the wind farm

GFM plant	Size of the SSD (MVA)	Q/V dSCR (pu/pu, based on SSD rating)	Q/V dSCRWF (pu/pu, based on wind farm rating)	Minimum stable grid SCR for wind farm with an SSD (based on wind farm rating)
GFM BESS from Project 1	150	2.53	1.9	1.1
GFM BESS from Project 2	30	3.71	0.55	2.45
Syncon	25	5.2	0.65	2.35

4.1.4 Time-domain verification using EMT simulations

In the above analysis, three SSD options were investigated to estimate their effectiveness in stabilising an existing wind farm with an unstable reactive power dynamic when connected to a grid with an SCR of less than 3. The estimate was derived arithmetically based on the dSCR values identified in Section 3 for each SSD, and the SCR withstand capability of the wind farm, without any time-domain EMT simulation. To complete the investigation, AEMO conducted EMT time-domain analysis to verify the above prediction, by reducing the grid SCR step-wise and examining at what grid SCR the wind farm would lose stability even with the SSD connected.

Figure 17 Time-domain verification using EMT studies for wind farm

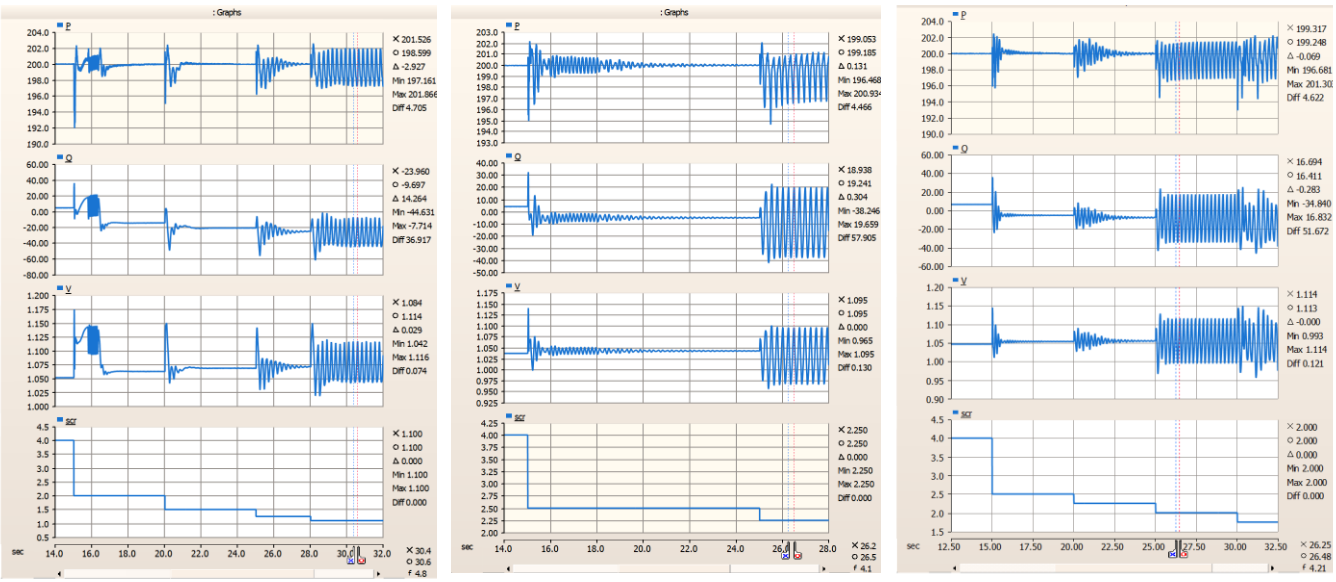

(a) (b) (c)

Figure 17(a) shows the wind farm behaviour when the grid SCR is gradually reduced from 4 to 1.1, with GFM BESS Project 1 connected in parallel. In previous simulations, the wind farm would lose stability as soon as the grid SCR drops to below 3. In **Figure 17(a)**, the wind farm is seen to maintain stability until the grid SCR drops to 1.1, where undamped oscillations start to manifest. This is equal to the minimum grid SCR requirement of 1.1 identified using the arithmetic method.

Figure 17(b) shows the wind farm behaviour when the grid SCR is gradually reduced from 4 to 2.25, with GFM BESS Project 2 connected in parallel. In **Figure 17(b)**, the wind farm is seen to maintain its stability until the grid SCR drops to 2.35, where undamped oscillations start to manifest. This is very similar to the minimum grid SCR requirement of 2.45 identified using the arithmetic method.

Figure 17(c) shows the wind farm behaviour when the grid SCR is gradually reduced from 4 to 1.75, with the synchronous condenser connected in parallel. In **Figure 17(c)**, the wind farm is seen to maintain its stability until the grid SCR drops to 2.25, where undamped oscillations start to manifest. This is very similar to the minimum grid SCR requirement of 2.35 identified using the arithmetic method.

Table 3 summarises the minimum required grid SCR to stabilise the wind farm with each SSD obtained from frequency scans-based approach and time-domain EMT simulations.

Table 3 Minimum grid SCR to stabilise wind farm: frequency scans-based approach versus EMT simulations

GFM plant	Minimum required grid SCR from frequency scans-based approach (based on wind farm rating)	Minimum required grid SCR for stability from time-domain EMT simulations (based on wind farm rating)
GFM BESS from Project 1	1.1	1.1
GFM BESS from Project 2	2.45	2.35
Syncon	2.35	2.25

As **Table 3** shows, the frequency scans-based approach documented in this technical note accurately estimated the minimum required grid SCR to stabilise wind farm for each assessed SSD. The minimum required grid SCR values obtained from this approach were within 5% of corresponding values derived from the time-domain EMT simulations.

4.1.5 Sizing of the SSD to stabilise the wind farm down to a specified grid SCR level

The arithmetic approach of assessing system strength support from an SSD can also be used to calculate the required size of each SSD to stabilise the wind farm at a specified grid SCR level. The size of the SSD to stabilise a generating plant at a certain SCR level, which is called the required minimum stable SCR, is given by:

$$Size\ of\ SSD = \left(\frac{minimum\ stable\ SCR\ -\ required\ minimum\ stable\ SCR}{dSCR_{SSD}}\right) \times IBR\ plant\ capacity, \qquad (4.2)$$

where

- minimum stable SCR refers to the SCR level that the generating plant remains stable on its own without needing the support of a SSD,
- required minimum stable SCR is a specific SCR level where the generating plant would otherwise be unstable without the system strength provided by the SSD, and
- dSCR is the dynamic SCR value of the SSD obtained in Section 3.

Equation 4.2 is derived through rearranging the terms in equation 4.1. **Table 4** summarises the required size of each different type of SSD[31] to stabilise the wind farm down to a grid SCR level of 1. The registered capacity of the IBR plant, which is the wind farm in this case study, is 200 MW.

[31] For example, the required size of GFM Project 1 to stabilise the wind farm down to a SCR level of 1 = $\left({(3-1)}/{2.53}\right) \times 200\ =\ 158\ MVA$

Table 4 Required size of each SSD to stabilise the wind farm at a grid SCR level of 1

Grid-forming resource	Q/V dSCR (pu/pu)	Size of the required SSD (MVA)
GFM BESS from Project 1	2.53	158
GFM BESS from Project 2	3.71	108
Syncon	5.2	77

Based on the values given in **Table 4**, the syncon has the smallest required size, while the GFM BESS from Project 1 has the largest. In fact, a GFM BESS from Project 1 would need to be twice as large to provide effective grid strength equivalent to that of the syncon.

4.2 Stabilisation of solar farm with active power instability

This section provides another case study of the arithmetic approach for a solar farm which has a different instability mechanism than the wind farm discussed in Section 4.1. The solar farm considered in this work has a registered capacity of 100 MW and, as shown in **Figure 18**, it is connected to the 66 kV high-voltage distribution network.

Figure 18 Single-line diagram of solar farm's connection to the network

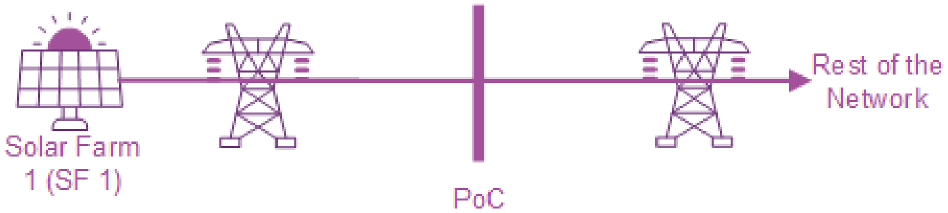

4.2.1 Analysis and identification of the instability for low SCR conditions

Figure 19 shows the results of the impedance-based stability analysis for the solar farm during a low irradiance condition[32]. During the impedance scan, the active power output of the solar farm was around 33 MW, although the active power setpoint (Pref) was at 60 MW under the grid conditions of SCR = 2.5 with an X/R ratio of 10. The impedance-based stability analysis reveals an instability mode around 19.5 Hz for a grid SCR below 2.5 with an X/R ratio of 10. The undamped resonance mode of the modal impedance[33] of $Z_m(s)$ shown in **Figure 19(a)** and the multivariable Nyquist plot's encirclement of the critical point, as shown in **Figure 19(b)** indicate that the solar farm has an internal unstable mode around 19.5 Hz.

[32] See https://www.aemo.com.au/-/media/files/initiatives/engineering-framework/2025/analysis-of-sub-synchronous-oscillation-in-west-murray-zone-power-system-in-australia---external.pdf for detailed analysis of this oscillation incident.

[33] The eigen values of the nodal impedance Zn(s) at each frequency point is called the modal impedance response and it is denoted as Zm(s).

Figure 19 Stability analysis of solar farm for a grid strength condition of SCR = 2.5 and X/R = 10

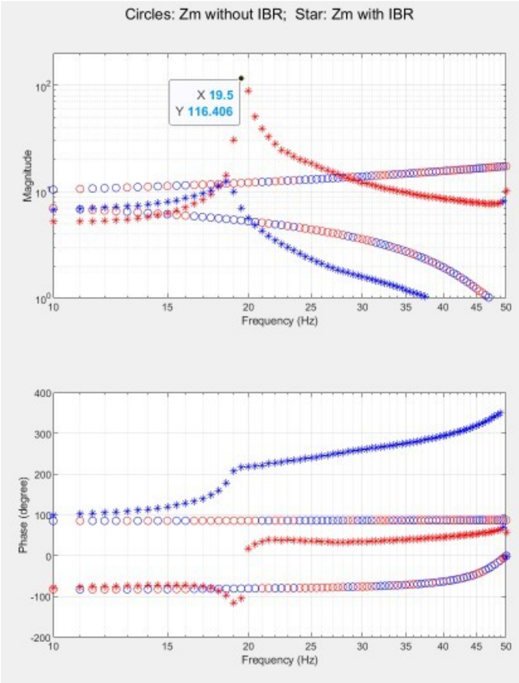

(a)

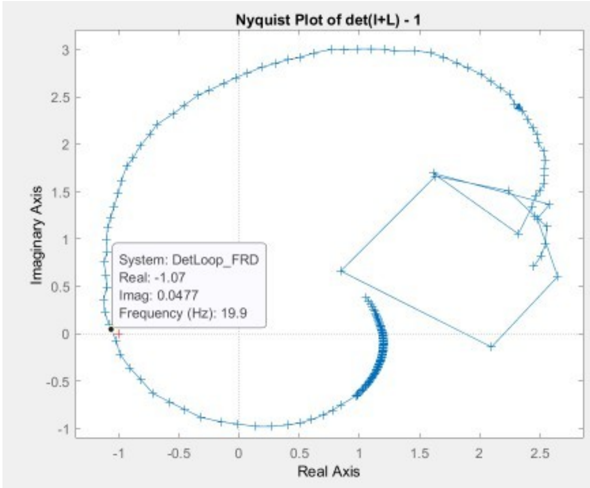

(b)

Similar to that done for the wind farm, a reduced-order analysis of the active power and reactive power dynamics was conducted in DQ domain to further understand the instability observed. **Figure 20(a)** shows the Nyquist plot of $Znet_{qd}$·$Yplant_{dq}$, which relates to the active power dynamics, and **Figure 20(b)** shows the Nyquist plot of $Znet_{qd}$·$Yplant_{qd}$, which relates to the reactive power dynamics. As shown in **Figure 20(a)**, the very close proximity of the Nyquist plot around 18 Hz to the critical point at (-1,0) signify reduced stability margins. This indicates a potential instability around 18 Hz within the active power dynamic of the solar farm.

Figure 20 Nyquist plot of (a) Znetqd*Yplantdq: Active Power Dynamics and (b) Znetdq*Yplantqd: Reactive Power Dynamics

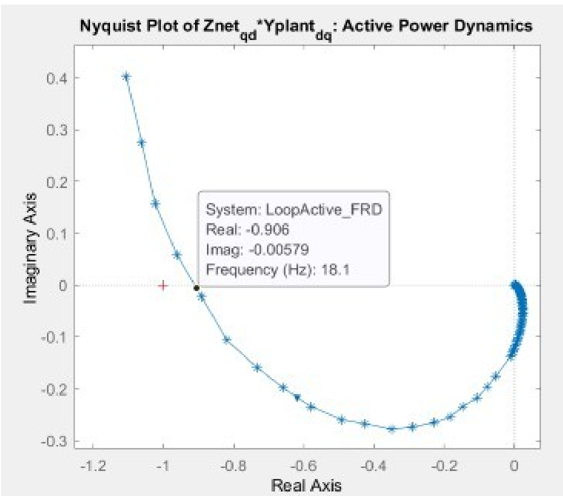

(a)

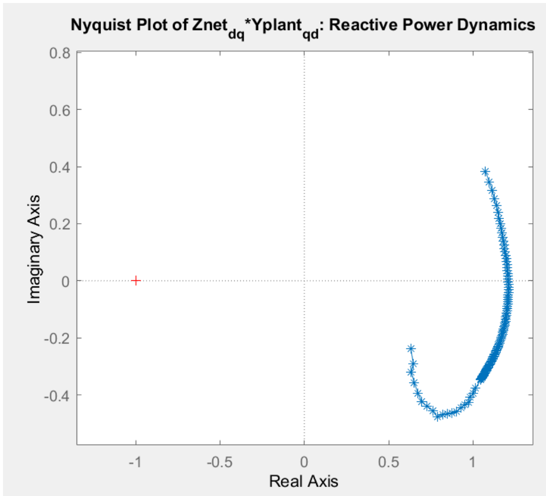

(b)

The DQ admittance matrix of the solar farm is shown in **Figure 21**. The findings from the reduced-order analysis are further confirmed by the reduced phase margin observed in the admittance response of Y_{dq} (subplot 12), as shown in **Figure 21**. Therefore, reduced-order analysis shows that the unstable mode around 18 Hz manifests in the active power control loop.

Figure 21 DQ admittance matrix of solar farm

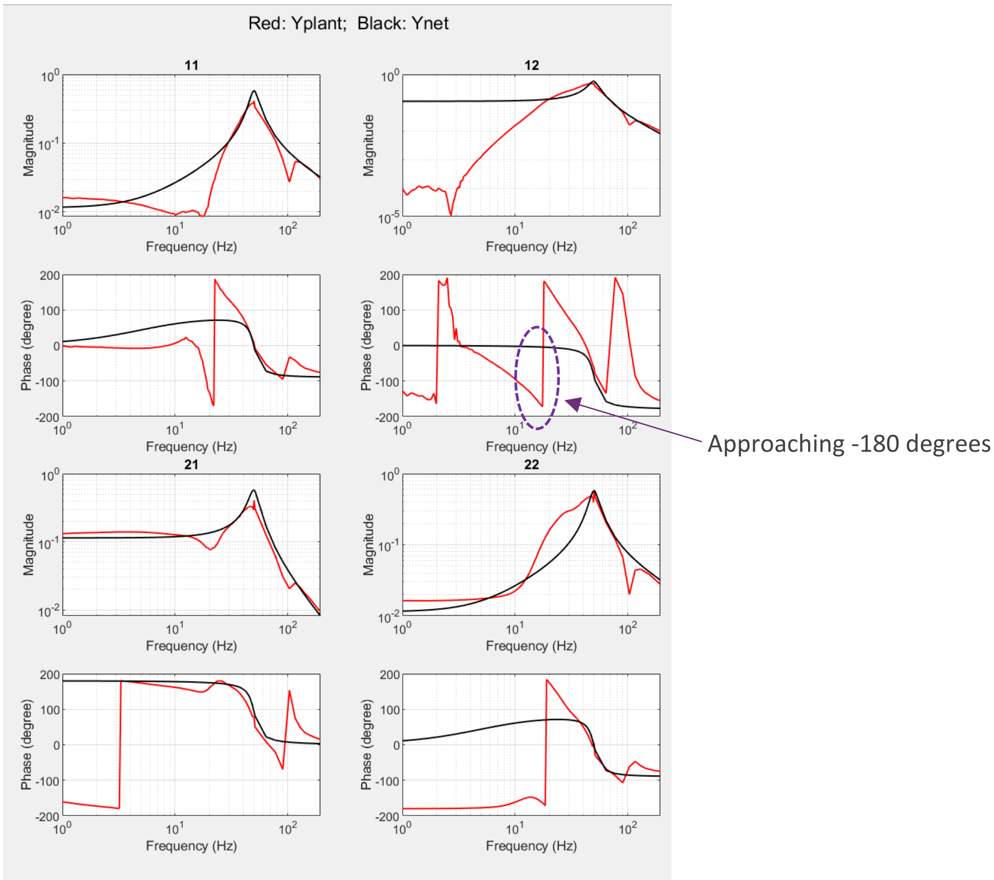

4.2.2 Validation of the identified instability mode in time-domain

The mode identified using impedance-based stability analysis was verified using time-domain EMT studies done in PSCAD™ utilising a SMIB setup.

Figure 22 shows the results of the time-domain results of the solar farm when the SCR is reduced from 4 to 1.5 in steps of 0.5 over 25 s. Each time the SCR is dropped by 0.5, oscillations are seen in solar farm active power, reactive power and connection point voltage immediately, however, they are adequately damped when the SCR is greater than or equal to 2.5. When the SCR is dropped below 2.5 at 25 s, oscillations are not adequately damped over the next 5 s, with the oscillation magnitude growing as the SCR is further reduced. The frequency of the oscillations is around 19.5 Hz. Therefore, the time-domain EMT simulations in PSCAD™ validate the admittance-domain findings of an inadequately damped mode around 19.5 Hz.

Figure 22 PSCAD™ results of solar farm when the SCR is reduced to 1.5 from 4

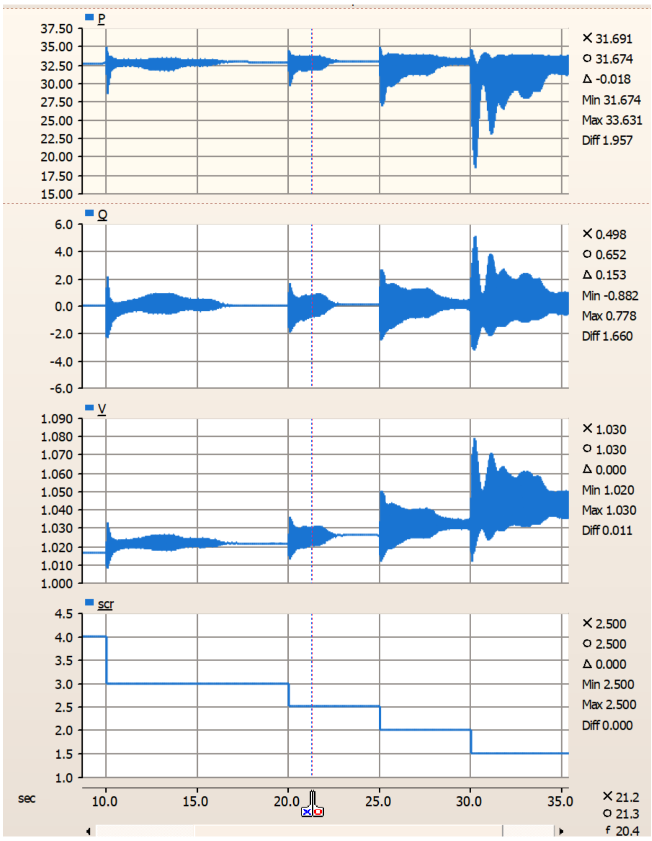

4.2.3 Quantification of system strength improvement by SSD for a solar farm

This section presents the analysis of using the SSDs discussed in Section 3 – two GFM BESS and one syncon – to stabilise the solar farm, using the arithmetic approach discussed in Section 4.1. **Figure 23** shows the parallel connection of the SSD to the solar farm's PoC.

Figure 23 The single-line diagram of the SSD's connection in parallel to the solar farm

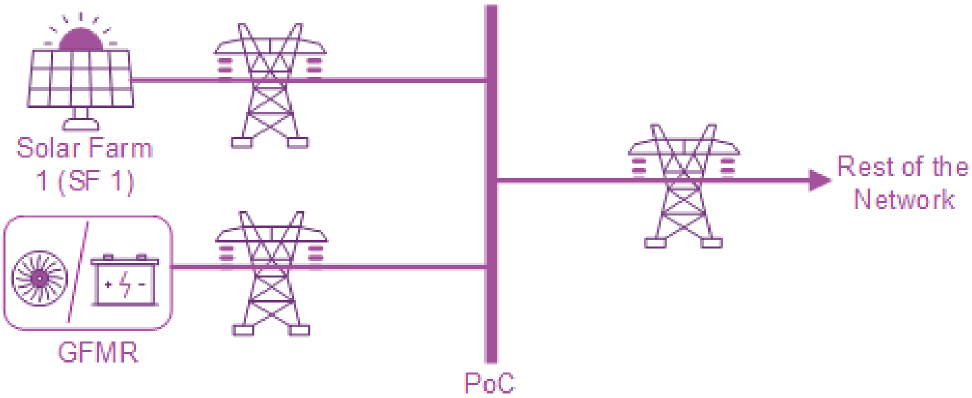

System strength provided by GFM BESS from Project 1

Recalling the grid strength contribution, or $dSCR_{P\theta}$, is 2.91 based on the 150 MVA rating of GFM BESS from Project 1. Applying Equation 4.1, the above $dSCR_{P\theta}$ can be expressed as $dSCR_{solar\ farm}$ based on the solar farm's rating, which is calculated to be 4.34. Given the solar farm requires a minimum grid SCR of at least 2.5 to remain stable operation, GFM BESS from Project 1 already provides an equivalent SCR of 4.34, therefore exceeds the minimum SCR required from the actual grid. In other words, with GFM BESS from Project 1 connected in parallel with the solar farm at the PoC, the residual grid SCR requirement for the solar farm to maintain stable operation will be zero.

System strength provided by GFM BESS from Project 2

Figure 5 earlier shows the grid strength contribution, or $dSCR_{P\theta}$, is 5.99 based on the 30 MVA rating of GFM BESS from Project 2. Applying Equation 4.1, the above $dSCR_{P\theta}$ can be expressed as $dSCR_{solar\ farm}$ based on the solar farm's rating, which is calculated to be 1.8. Given that the solar farm requires a minimum grid SCR of at least 2.5 to maintain stable operation, with GFM BESS from Project 2 providing an equivalent SCR of 1.8, the grid still needs to provide a SCR of 0.7, for the solar farm to remain stable.

System strength provided by synchronous condenser

Figure 7 earlier shows the grid strength contribution, or $dSCR_{P\theta}$, is 7.28 based on the 25 MVA rating of the syncon. Applying Equation 4.1, the above $dSCR_{P\theta}$ can be expressed as $dSCR_{solar\ farm}$ based on the solar farm's rating, which is calculated to be 1.82. Given that the solar farm requires a minimum grid SCR of at least 2.5 to remain stable operation, with a syncon providing an equivalent SCR of 1.82, the grid still needs to provide an SCR of 0.68 for the solar farm to maintain stable operation.

Table 5 summarises the dSCR and $dSCR_{solar\ farm}$ provided by each SSD and the minimum grid SCR level that the solar farm can stably operate at with each SSD connected.

Table 5 Summary of the dSCR provided by each SSD to stabilise the solar farm

GFM plant	P/θ dSCR (pu/pu, based on SSD rating)	P/θ $dSCR_{solar\ farm}$ (pu/pu, based on solar farm rating)	Minimum stable grid SCR for solar farm with a SSD (based on solar farm rating)
GFM BESS from Project 1	2.91	4.34	0 (effectively no further grid support required)
GFM BESS from Project 2	5.99	1.8	0.7
Syncon	7.28	1.82	0.68

4.2.4 Time-domain verification using EMT simulations

EMT time-domain analysis has been conducted to verify the above predictions, by reducing the grid SCR step-wise and examining what grid SCR the solar farm would lose stability even with the SSD connected.

Figure 24(a) shows the EMT time-domain simulation results, when the grid SCR is gradually reduced from 3.0 to 0.5, with GFM BESS from Project 1 connected in parallel with the solar farm. In previous simulations, the solar farm would lose stability as soon as the grid SCR drops below 2.5. In **Figure 24(a)**, the solar farm is seen to maintain stability even once the grid SCR drops to 0.5, indicating the significant equivalent system strength provided by the GFM BESS from Project 1.

Figure 24(b) shows the EMT time-domain simulation results, where the grid SCR is gradually reduced from 2.0 to 0.5, with GFM BESS from Project 2 connected in parallel with the solar farm. In **Figure 24(b)**, the solar farm is seen to maintain stability until the grid SCR falls to 0.5, where the oscillation start to manifest. This is very close to the minimum grid SCR requirement of 0.7 identified using the arithmetic method.

Figure 24(c) shows the EMT time-domain simulation results, where the grid SCR is gradually reduced from 3.0 to 0.5, with the syncon connecting in parallel with solar farm. In previous simulations, the solar farm would lose stability as soon as the grid SCR drops below 2.5. In **Figure 24(c)**, the solar farm is seen to maintain its stability even with the grid SCR dropping to 0.5, highlighting the significant equivalent system strength support provided by the syncon.

Table 6 summarises the required minimum grid SCR to stabilise the solar farm with each SSD obtained from frequency scans-based approach and verified through time-domain EMT simulations.

Figure 24 Time-domain verification using EMT studies for wind farm

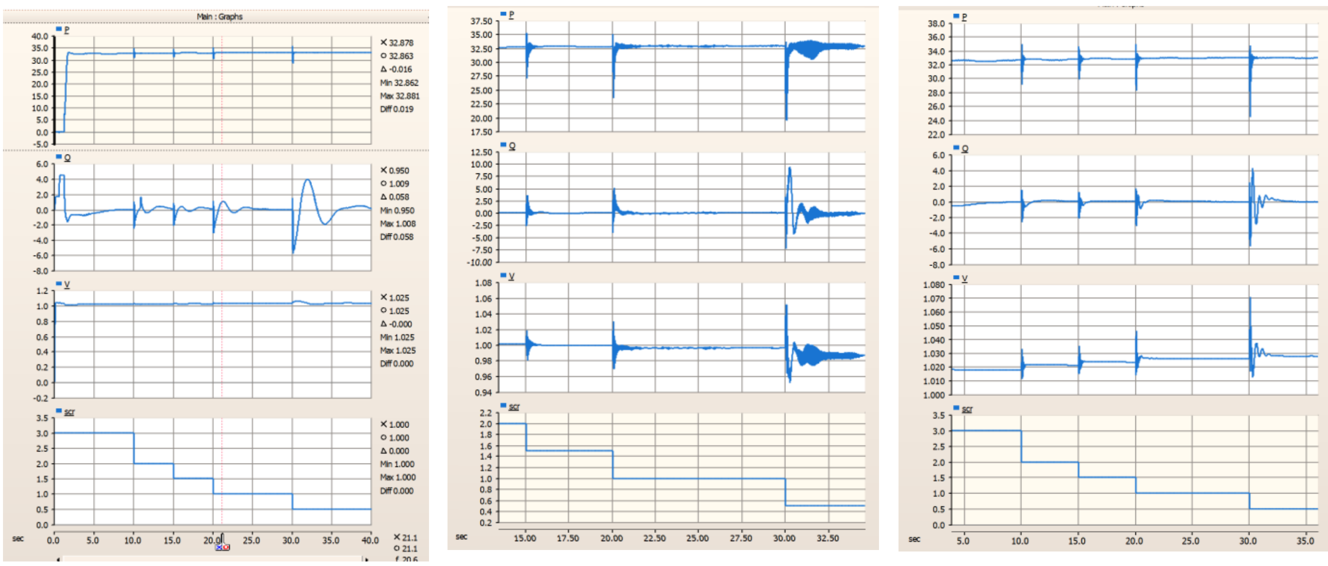

(a) (b) (c)

Table 6 Required grid SCR to stabilise the solar farm: frequency scans-based approach versus EMT simulations

GFM plant	Required minimum grid SCR from frequency scans-based approach (based on solar farm rating)	Required minimum grid SCR for stability from time-domain EMT simulations (based on solar farm rating)
GFM BESS from Project 1	0	-*
GFM BESS from Project 2	0.7	0.7
Syncon	0.7	0.5

* Occurrence of negative SCR values is impractical in real life grids, therefore negative SCR values were not modelled in the EMT simulation. Hence, the required grid SCR for stability could not be verified with EMT simulations. However, solar farm remains stable even if the grid SCR is dropped down to as low as 0.5, indicating the required grid residual SCR with GFM BESS from Project 1 is significantly low.

As shown in **Table 6**, the frequency scans-based approach documented in this report can reasonably estimate the minimum required grid SCR to stabilise the solar farm with each SSD option discussed in Section 3. The minimum required grid SCR values obtained from this approach are equal or reasonably close to those from the time-domain EMT simulations in the verifiable cases.

4.2.5 Sizing of the SSD to stabilise the solar farm down to a specified grid SCR level

Equation 4.2 was used to calculate the required size of each different type of SSD[34] to stabilise the solar farm down to a grid SCR level of 1. **Table 7** summarises the required size of each different type of SSD. The registered capacity of the IBR plant, which in this case is the solar farm, is 100 MW.

Table 7 Required size of each SSD to stabilise solar farm at a grid SCR level of 1

GFM plant	P/θ dSCR (pu/pu)	Size of the required SSD (MVA)
GFM BESS from Project 1	2.91	52
GFM BESS from Project 2	5.99	25
Syncon	7.28	21

Based on the values given in **Table 7**, the syncon has the smallest required size, while the GFM BESS from Project 1 has the largest. In fact, a GFM BESS from Project 1 would need to be roughly twice as large to provide grid the equivalent strength to that of the syncon. The required size of GFM BESS from Project 2 to stabilise the solar farm at a SCR level of 1 is roughly equal to that of the syncon.

4.3 Case study summary

Section 4 of this report presents two case studies, where the system strength provision of three SSDs were quantified for a GFL wind farm and solar farm, using the arithmetic approach documented in this report, and further verified via EMT time-domain simulations. The case studies started by identifying the inherent instability mechanisms in each GFL IBR plant, and boundary grid conditions where such instability could manifest. Then the system strength provision assessment was conducted entirely based on simple arithmetic calculations, relying on the system strength Jacobian obtained from frequency domain scan approach described in Section 3.

The case studies highlighted the effectiveness of the arithmetic approach in providing early prediction of whether a certain system strength remediation scheme would achieve its purpose, without lengthy EMT time-domain analysis. It shows great potential to serve as a screening tool for subsequent EMT time-domain simulations, to focus such simulations on a small set of grid conditions, which could reduce the study scope for system strength remediation schemes by a considerable amount.

The arithmetic approach may also be used to predict the necessary size of a system strength remediation scheme involving SSDs (GFM BESS or syncons), based on early knowledge of a project’s guaranteed minimum stable SCR, and a minimum SCR provided by the grid at the proposed connection point. This can be done even without a detailed model of the new IBR to be connected.

This could provide valuable information for project developers to undertake an early assessment of likely remediation options and costs, allowing them to make an informed decision on the most appropriate connection pathway.

[34] For example, the required size of GFM Project 1 to stabilise the solar farm down to a SCR level of 1 = $\left({(2.5-1)}/{2.91}\right) \times 100 = 52\ MVA$

5 Conclusion

The system strength Jacobian provides a frequency-domain basis for quantifying the dynamic system strength support contributed by SSDs. Since it can be derived directly from frequency-domain scans, it integrates well with existing system strength assessment using vendor-specific black-box EMT PSCAD™ models. Moreover, it provides an intuitive interpretation of system strength by capturing the sensitivity of active and reactive power to variations in voltage angle and magnitude, thereby providing valuable insights into the dynamic behaviour and small-signal stability analysis of IBRs and power systems more broadly.

The system strength Jacobian was used to characterise the voltage source behaviour of SSDs. The gains of $P/\theta(s)$ and $Q/V_m(s)$ from the system strength Jacobian of each SSD over the frequency range of interest were used to quantify their system strength provisions. The system strength Jacobians of two GFM BESS and a syncon were obtained through frequency domain scans.

The system strength Jacobian-based approach also facilitates the indicative sizing of SSDs to address known small-signal stability issues of GFL IBRs which are related to system strength. These issues are mitigated by supplementing the system strength support at the IBR connection point through the parallel integration of an SSD. The report applied this approach to quantify the effectiveness of a syncon and two GFM BESS in mitigating the stability issues associated with a GFL wind farm and solar farm.

It must be noted that these results are specific to the models, ratings, operating points, control settings and evaluation frequencies considered in this report. They should not be generalised to conclude that one technology type inherently provides stronger system strength support than another. The results also suggest the equivalence between system strength support from syncons and GFM BESS are not universal, and it can depend on OEM-specific implementation and settings. The proposed method provides a pathway to assess this equivalence more transparently and can help inform future planning assumptions.

This report also discusses the relationship between conventional system strength metrics, such as SCR, and dSCR. The proposed method provides a framework for linking traditional SCR-based practice with dynamic stability analysis by expressing SSD support as an SCR-like dynamic contribution. This allows stability issues that are traditionally characterised using SCR to be assessed with additional information about the frequency-dependent dynamic support provided by SSDs. However, the dSCR-based approach reflects aspects of dynamic system strength support that are not captured in a steady-state, fault-level-based SCR calculation.

The dSCR values derived from a system strength Jacobian may be used to predict the necessary size of a system strength remediation scheme involving SSDs (GFM BESS or syncons) based on early project knowledge, such as the guaranteed minimum stable SCR for their IBR devices and a minimum connection point SCR. This information is obtainable even without the detailed model of the new IBR to be connected. The findings could therefore provide valuable information for project developers and relevant stakeholders for an early assessment of likely remediation options and cost, allowing them to make an informed decision on the most appropriate connection pathway.

The method should not be interpreted as a replacement for detailed EMT assessment or final connection studies. The calculated dSCR values depend on the SSD model, rating, tuning, operating point, and should be used with appropriate frequency range and targeted instability mechanism. Targeted EMT validation would still be required where the results are used to support project-specific decisions, confirm large-signal performance, or assess broader power system security requirements.

Within these limitations, the proposed system strength Jacobian and dSCR framework appears to offer a useful and robust baseline for targeted EMT analyses and thus improves the efficiency of early-stage system strength remediation studies.

AEMO will continue targeted engagement with relevant internal teams, TNSPs and other stakeholders to test the method through suitable planning and connection applications. This work will further assess the method across a broader range of device designs, operating conditions and network conditions, and evaluate its use for early screening, comparison and indicative sizing of system strength remediation options to help focus detailed EMT assessments on the most credible solutions. Project-specific EMT studies will remain necessary to validate applications of the method.

A1. Appendix

The following sections provide the derivation of the system strength Jacobian and further analysis of the frequency-domain response of the system strength Jacobian.

A1.1 Characteristics of ideal voltage source behind an impedance

The frequency-domain characteristics of an ideal voltage source is firstly investigated to provide a benchmark for assessing the behaviour of SSDs, primarily focusing on their P and Q response against changes in θ and V_m at the connection point, respectively. As shown in **Figure 25**, an ideal voltage source (V_i) behind a reactance (L) with an internal resistance (R) connected to the grid (V_g) at its PoC is considered to characterise the behaviour of an ideal voltage source in the frequency-domain.

Figure 25 An ideal voltage source behind a reactance connected to the grid

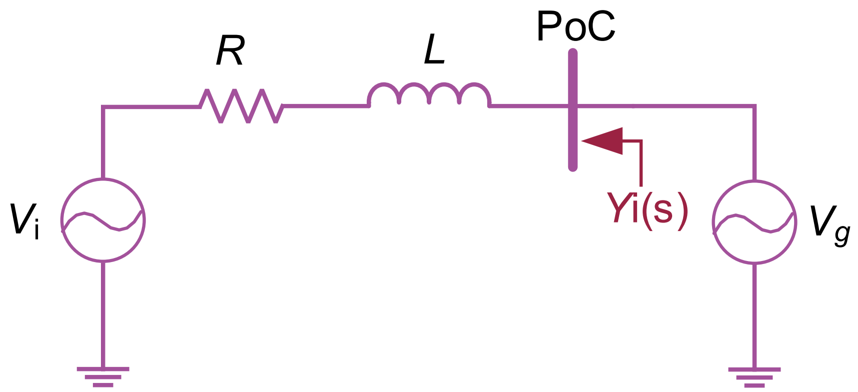

The Direct-Quadrature (DQ) admittance of the voltage source V_i when viewed from its PoC, which is denoted as $\boldsymbol{Y}_i(s)$, can be derived as:

$$\boldsymbol{Y}_i(s) = \begin{bmatrix} Y_{dd}(s) & Y_{dq}(s) \\ Y_{qd}(s) & Y_{qq}(s) \end{bmatrix} = \frac{1}{(R+sL)^2 + (\omega_1 L)^2} \begin{bmatrix} R+sL & \omega_1 L \\ -\omega_1 L & R+sL \end{bmatrix}$$

where "s" is the Laplace operator and ω_1 is the nominal frequency in rad/s. For small perturbations in the PoC voltage, the DQ components of the voltage at the PoC ($V_d(s)$ and $V_q(s)$), respectively, are related to the magnitude ($V_m(s)$) and phase ($\theta(s)$) of the PoC voltage as:

$$V_m(s) = V_d(s)$$

and

$$\theta(s) = {V_q(s)}/{V_1}$$

where V_1 is the peak of the three-phase voltage at the PoC. Using these relationships, the linearised transfer function from the PoC voltage magnitude $V_m(s)$ and phase $\theta(s)$, to the active power $P(s)$, and reactive power $Q(s)$, at the PoC is derived as:

$$\begin{bmatrix} P(s) \\ Q(s) \end{bmatrix} = \begin{bmatrix} \frac{P_0}{V_1} - \frac{3}{2} V_1 \cdot Y_{dd}(s) & -\frac{Q_0}{V_1} - \frac{3}{2} V_1 \cdot Y_{dq}(s) \\ \frac{Q_0}{V_1} + \frac{3}{2} V_1 \cdot Y_{qd}(s) & \frac{P_0}{V_1} + \frac{3}{2} V_1 \cdot Y_{qq}(s) \end{bmatrix} \begin{bmatrix} V_m(s) \\ V_1 \cdot \theta(s) \end{bmatrix}$$

where P_0 and Q_0 are the steady-state active and reactive power output into the grid at the PoC, respectively.

This 2x2 transfer function matrix is referred to as the system strength Jacobian in this report[35,36,37,38]. The term $V_1 \cdot \theta(s)$ is considered in the right most matrix instead of $\theta(s)$ to simplify the comparison between the transfer functions in the system strength Jacobian and it helps relate the active and reactive-power response terms to a common voltage perturbation basis.

A1.2 Interpreting the system strength Jacobian

The system strength Jacobian provides a frequency-domain representation of how a voltage source responds to small changes in voltage magnitude and voltage angle at the PoC. In this report, this response is used to characterise voltage-source-like behaviour relevant to system strength support.

From the above system strength Jacobian, two relevant transfer functions are considered in this report:

- the reactive power response to voltage magnitude perturbations, $Q/V_m(s)$, and
- the active power response to voltage angle perturbations, expressed on the voltage-equivalent basis as P/(V1·θ(s)).

These two transfer functions are used because they represent the main direct relationships between voltage perturbations and power response in the Jacobian. They therefore provide a basis for comparing the dynamic system strength support capability of different SSDs.

To illustrate how the system-strength Jacobian represent ideal voltage source behind reactance behaviour, this report considered a steady-state operating condition in which Q_0 is small. Under this condition, both P/(V1·θ(s)) and $Q/V_m(s)$ transfer functions exhibit similar low-frequency magnitudes and approximately 180° phase difference. The subsequent demonstration then used $Q/V_m(s)$ as a representative transfer function for both P/(V1·θ(s)) and $Q/V_m(s)$, since the two transfer functions are highly similar for frequencies below 50 Hz for the considered operating condition. It should be noted that the Jacobian-based system-strength quantification method is not limited to the operating conditions assumed here; as discussed later in this section, the method remains valid for any operating condition of the SSD.

As an example, **Figure 26** shows the frequency-domain response of the system strength Jacobian for an ideal voltage source behind an impedance. The impedance is considered to have a resistance R = 0.075 Ω, and an inductance L = 0.72 mH, while the peak phase voltage of the voltage source is V_1 = 0.56 kV. This impedance correspond to an SCR of 2 based on 1 MVA and 0.69 kV system bases.

[35] For the full derivation of the system strength Jacobian, see Shah, Shahil, Weihang Yan, Przemyslaw Koralewicz, Vahan Gevorgian, Deepak Ramasubramanian, Robb Wallen, Anderson Hoke, Benjamin Kroposki, and Barry Mather, 2023, "A Testing Framework for Grid-Forming Resources", at https://www.nlr.gov/docs/fy23osti/84604.pdf.

[36] Frequency Scans for GFM Performance Verification – 2024 IEEE Power and Energy Society General Meeting, https://www.nlr.gov/docs/fy25osti/90780.pdf.

[37] Frequency Scans for GFM Performance Verification, 2023 IEEE Power and Energy Society General Meeting, https://www.nlr.gov/docs/fy23osti/87061.pdf.

[38] GFM Inverter Hardware Testing – 2024 ESIG Spring Technical Workshop, https://www.nlr.gov/docs/fy24osti/89421.pdf.

Figure 26 Frequency-domain response of the system strength Jacobian for an ideal voltage source behind reactance

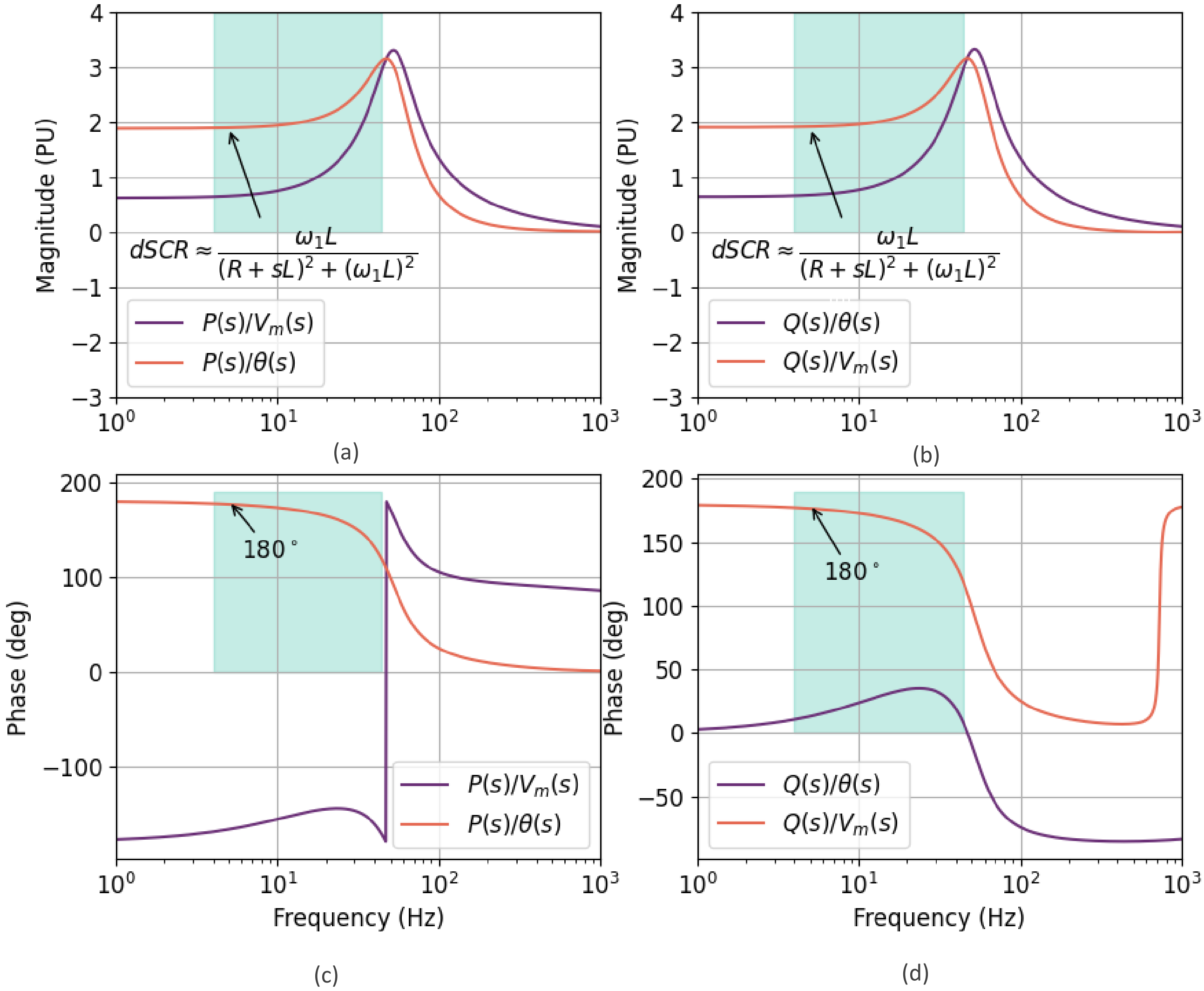

From **Figure 26(b)**, the Q/Vm(s) transfer function has a frequency response similar to a second order low-pass filter which has a cutoff frequency around 50 Hz. Therefore, the frequency range of interest in this study is below 50 Hz, with a primary focus on the 4-40 Hz band, allowing for a sufficient margin as shown in the teal area in **Figure 26(b)** and **Figure 26(d)**. As shown in **Figure 26(d)**, the phase below the corner frequency is around 180 degrees, and as shown in **Figure 26(b)**, the steady-state gain of $Q/V_m(s)$ is $(-3/2)*(\omega_1 L/((R+sL)^2+(\omega_1 L)^2))$.

As the phase of both $P/(V_1 \cdot \theta(s))$ and $Q/V_m(s)$ is 180 degrees within the frequency range of interest (4-40 Hz), small changes in angle and voltage magnitude can lead to P and Q responses from the ideal voltage source. These response disturbances are 180 degrees out of phase with the angle and voltage magnitude changes, therefore would oppose such changes. In other words, the ideal voltage source actively opposes variations in phase angle and voltage magnitude within the frequency range associated with sub-synchronous oscillations and maintains a stable voltage waveform. At higher frequencies, where this phase relationship no longer provides effective compensation, the gain of $P/(V_1 \cdot \theta(s))$ and $Q/V_m(s)$ are sufficiently low that their impact is negligible.

Based on above analysis, the frequency-domain characteristics of system strength Jacobian of an ideal voltage source defines the P and Q response of that voltage source against the voltage angle and magnitude changes. As such, the voltage source behaviour can be characterised by using the $Q/V_m(s)$ and $P/\theta(s)$ transfer functions in the system strength Jacobian. The same $Q/V_m(s)$ and $P/\theta(s)$ transfer function characteristics obtained from an SSD can also be used to benchmark against those of the ideal voltage source illustrated in **Figure 26**, and thereby enables the quantification of the system strength provided by an SSD.

A1.3 Dynamic short-circuit ratio (dSCR)

This report defines a dSCR as a numerical indicator derived from the frequency-domain response of the system strength Jacobian.

This relationship can be extended to define the dSCR to quantify the system strength provided by an SSD[39,40,41,42,43]. Similar to the ideal voltage source, the dSCR of an SSD is defined by the per-unit gain of $Q/V_m(s)$ and $P(s)/\theta(s)$ transfer functions within the frequency band of interest (4-40 Hz used in this report).

Two dSCR values can be calculated depending on the transfer function:

- $dSCR_{QV}$ based on the magnitude of the $Q/V_m(s)$ transfer function, and
- $dSCR_{P\theta}$ based on the magnitude of the $P/\theta(s)$ transfer function.

These two values reflect that active and reactive-power dynamic support may not be identical for a given SSD. Where both values are relevant to the studied phenomenon, they should be assessed separately.

For a specific SSD, the dSCR value can be derived using different approach from the transfer function magnitude, include using the lowest magnitude, an average magnitude, or another representative value across the frequency band. The selected approach must be stated clearly because it affects the resulting dSCR value.

In this report, the dSCR of an SSD used in cross-device comparison is obtained from the lowest magnitude of its $Q/V_m(s)$ and $P/\theta(s)$ transfer functions within the common 4-40 Hz assessment band, or within a narrower frequency band where the SSD exhibits voltage source behaviour. The frequency at which this minimum occurs is reported with each value. The dSCR values calculated in this report are case-specific indicators, and they should not be interpreted as universal capability values for the SSD across all operating conditions, network conditions or instability mechanisms.

It is worth mentioning that narrow spikes in the magnitude response over a narrow band of frequencies should be avoided when determining the dSCR, as such spikes may otherwise lead to underestimation or overestimation of the SSD's system strength contribution.

---

[39] Shah, Shahil, Weihang Yan, Przemyslaw Koralewicz, Vahan Gevorgian, Deepak Ramasubramanian, Robb Wallen, Anderson Hoke, Benjamin Kroposki, and Barry Mather. "A Testing Framework for Grid-Forming Resources" (IEEE Power & Energy Society General Meeting. Orlando, July 2023).

[40] Energy Systems Integration Group's GFM Testing Project Team. "Testing the Performance of Grid-Forming Resources" (Energy Systems Integration Group. Online, September 2025).

[41] Shah, Shahil, Przemyslaw Koralewicz, Vahan Gevorgian, Weihang Yan, Robb Wallen, Emanuel Mendiola. Frequency Scans for GFM Performance Verification (IEEE Power & Energy Society General Meeting. Orlando, July 2023).

[42] Shah, Shahil, Przemyslaw Koralewicz, Vahan Gevorgian, Weihang Yan, Robb Wallen, Emanuel Mendiola. Frequency Scans for GFM Performance Verification (IEEE Power & Energy Society General Meeting. Seattle, July 2024).

[43] GFM Inverter Hardware Testing – 2024 ESIG Spring Technical Workshop, https://www.nlr.gov/docs/fy24osti/89421.pdf.

Further, to quantify the system strength support of an SSD, dSCR values should be determined for each operating point within the SSD's operating envelope. This allows evaluation of whether the SSD's contribution to dSCR changes across its operating range. Where variation exists, the minimum dSCR contribution over the operating range is used to ensure a conservative estimate.

The methodology used to quantify the system strength provided by SSD is summarised as follows:

- Step 1: the system strength Jacobian of SSDs are obtained using the frequency-domain impedance scans[44].
- Step 2: the relevant transfer functions in the system strength Jacobian are assessed over the frequency range of interest, for each $Q/V_m(s)$ and $P/\theta(s)$ transfer functions in the system strength Jacobian.
- Step 3: the per-unit magnitudes of the selected transfer functions are used to derive dSCR values.
- Step 4: the calculated dSCR values provide a common numerical basis for comparing the dynamic system strength support capability of different SSDs under the studied assumptions.

[44] For more details on obtaining the admittance-based frequency scans see Analysis of Sub-synchronous Oscillations in West Murray Zone Power System in Australia, https://www.aemo.com.au/-/media/files/initiatives/engineering-framework/2025/analysis-of-sub-synchronous-oscillation-in-west-murray-zone-power-system-in-australia---external.pdf?rev=91a3c919b83246b7b24835f0339b85e6&sc_lang=en.